Developmental prosopagnosics have widespread selectivity reductions across category-selective visual cortex

Guo Jiahui[a,1], Hua Yang[a], and Bradley Duchaine[a]

[a]Department of Psychological and Brain Sciences, Dartmouth College, Hanover, NH 03755

Developmental prosopagnosia (DP) is a neurodevelopmental disorder characterized by severe deficits with facial identity recognition. It is unclear which cortical areas contribute to face processing deficits in DP, and no previous studies have investigated whether other category-selective areas function normally in DP. To address these issues, we scanned 22 DPs and 27 controls using a dynamic localizer consisting of video clips of faces, scenes, bodies, objects, and scrambled objects. We then analyzed category selectivity, a measure of the tuning of a cortical area to a particular visual category. DPs exhibited reduced face selectivity in all 12 face areas, and the reductions were significant in three posterior and two anterior areas. DPs and controls showed similar responses to faces in other category-selective areas, which suggests the DPs' behavioral deficits with faces result from problems restricted to the face network. DPs also had pronounced scene-selectivity reductions in four of six scene-selective areas and marginal body-selectivity reductions in two of four body-selective areas. Our results demonstrate that DPs have widespread deficits throughout the face network, and they are inconsistent with a leading account of DP which proposes that posterior face-selective areas are normal in DP. The selectivity reductions in other category-selective areas indicate many DPs have deficits spread across high-level visual cortex.

face perception | visual recognition | developmental disorder | prosopagnosia | scene perception

Individuals with developmental prosopagnosia (DPs) have great difficulty with facial identity recognition despite normal low-level vision, normal intelligence, and no history of brain damage (1, 2). DPs' problems with faces are a significant social handicap and can lead to chronic social anxiety (3, 4). Although neural differences between DPs and participants with normal face recognition have been identified, fundamental issues concerning the neural basis of DP remain unclear. These questions include (*i*) which regions in the face-processing system function abnormally in DP, (*ii*) whether areas outside the face processing system contribute to DPs' deficits with faces, and (*iii*) whether DPs show functional abnormalities in response to categories other than faces. Here we address these questions by presenting controls and a relatively large group of DPs with videos of faces and other categories and then comparing the selectivity of their responses.

Facial identity recognition depends on a set of face-selective cortical regions that extend from the occipital lobe to the anterior temporal lobe (5–7), and the location of DPs' neural deficits within the face network is controversial. One view proposes DP results from a disconnection between posterior face-selective areas and anterior face-selective areas (8, 9). Support for this view comes from findings suggesting posterior face areas function normally in DPs (10–12), whereas white matter tracts in DPs linking posterior and anterior face areas are compromised (13) and anterior temporal areas in DPs exhibit reduced activation (8, 10) as well as reduced structural integrity (14). However, an alternative view suggests DPs have deficits in both posterior and anterior face-selective areas. This distributed account is supported by the findings indicating anterior abnormalities, in combination

with studies indicating DPs have reduced face selectivity (15, 16) and functional connectivity in posterior face-selective areas (17–19) as well as structural abnormalities in the vicinity of posterior face areas (14, 15). In addition, two recent studies of white matter tracts in DP found deficits local to ventral temporal face areas but no abnormalities in long-range tracts linking posterior and anterior face areas (20, 21). Because the findings reviewed above, particularly the fMRI studies, paint an inconsistent picture, often used small samples, and did not investigate the entire face-processing system, it is critical to thoroughly compare anterior and posterior face areas in a large group of DPs.

fMRI investigations of DP have focused solely on face-selective areas, but we believe it is also essential to examine responses in areas selective for other visual categories. The response of these areas to their preferred categories (e.g., scene selectivity in scene areas) will shed light on the extent of the cortical anomalies associated with DP and may provide insight into the developmental processes that lead to DP. Face input to the visual system early in life appears to be necessary for normal face recognition later in life (22, 23), and it has been hypothesized DP may result from a lack of exposure to faces early in life (24, 25), possibly due to deficits in subcortical mechanisms that lead infants to preferentially attend to faces (26). If DP results from inadequate face input in the context of normal exposure to other categories, DPs would be expected to show impairments only in face-selective areas while other category-selective areas should respond normally to preferred categories. However, if non-face category-selective areas respond abnormally in many DPs, it would suggest DP often results from impairments to neurobiological

---

Significance

People with developmental prosopagnosia (DP) have extremely poor face recognition and even have problems recognizing the faces of family and close friends. We carried out a comprehensive investigation of the neural basis of DP by comparing brain responses to multiple visual categories in DPs and people with normal face processing. The DPs showed widespread abnormalities in areas specialized for face processing and areas that respond preferentially to scenes and bodies. The abnormalities in scene and body areas indicate cortical problems in many DPs extend beyond face areas and open the door to investigations of developmental disorders impacting recognition of categories other than faces.

factors with broader effects rather than insufficient experience with faces. An event-related potential study indicated DPs have abnormal neural responses to bodies (27), but the responses of nonface category-selective areas in DP have not been examined.

To address the issues discussed above, we carried out a systematic analysis of category selectivity in DP. We first compared the distribution of category selectivity in DPs and controls using whole-brain results. Then, to more precisely quantify the selectivity differences, we adopted a data analysis approach we refer to as the "variable window" method to conduct group comparisons of selectivity in category-selective areas that were individually defined for each participant (28, 29). For each region of interest (ROI), we first created an anatomical mask around the expected location for all participants. To compare results at a variety of ROI sizes, we then computed the percent signal change to different categories across a range of selectivity percentages within the mask (top 5%, top 10%, etc.) for each individual. This method provides an objective means to generate individualized functionally defined ROIs. It also avoids omitting results from participants with responses below typically used threshold and fairly compares selectivity between groups that often have unequal cluster sizes (16, 30).

Materials and Methods

Participants. Twenty-two DPs (seven males, mean age 41.9 y) and 25 typical adults (10 males, mean age 42.3 y) participated in the study. DPs were recruited from www.faceblind.org, and all reported problems in daily life with face recognition. To assess their face recognition, DPs were tested with the Cambridge Face Memory Test (CFMT) (31), a famous face test (32), and an old–new face discrimination test (32). All DPs except one performed two or more SDs below the mean of published control results in at least two of the three diagnostic tests (33, 34). The DP who did not reach −2 SD on two tests scored poorly on two of the three tasks (CFMT: z = −1.9; famous face: z = −7.1; old–new: z =−0.5), so we included her to increase the sample size. *SI Appendix*, Fig. S1A shows the Z-score of all DPs on the three diagnostic tests. All participants had normal or corrected-to-normal vision (*SI Appendix*, Table S2) and had no current psychiatric disorders. Participants provided written informed consent before doing the tasks, and all procedures were approved by Dartmouth's Committee for the Protection of Human Participants.

Stimuli and Procedures. Participants did a one-back task during a dynamic localizer scan containing five visual categories (faces, scenes, bodies, objects, and scrambled objects). Stimuli in the localizer were brief video clips of each category. Face and object stimuli were obtained from video clips in Fox et al. (35), scene and body video clips came from Pitcher et al. (36), and scrambled objects were created by scrambling the video clips of the objects spatially into 24 × 16 grids. Each video clip subtended ~18.5° × 12.3° of visual angle for width and height.

Each participant completed five scans. Each scan comprised 10 12-s category blocks of video clips interleaved with 12-s fixation blocks, which in total lasted about 4.2 min. Each visual category was displayed twice in each scan in a quasi-random order across scans. In each category block, six 1,500-ms video clips were presented interleaved by blank fixation screens presented for 500 ms (*SI Appendix*, Fig. S1B). Stimuli were presented using Superlab 4.5.3 (www.superlab.com/) and displayed to the participant via a PanasonicDT-4000UDLP projector (resolution: 1,024 × 768; refresh rate: 60 Hz) at the rear of the scanner.

Leave One Run Out. The five runs were divided into localization runs and test runs to carry out a "leave-one-out" analysis (28, 29). In each of the leave-one-out combinations, four of the five runs for a participant were used to localize the voxels that showed the strongest preference for the preferred category (e.g., largest z-value for faces > objects contrast). To avoid the double-dipping problem (37), the responses of the selected voxels to each stimulus condition were then measured in the left-out run. All five combinations were analyzed and then averaged to produce the final result for each participant.

Category Selectivity. Category selectivity was used to measure how strongly tuned a cortical area was to a particular category. Selectivity for faces was defined as the difference between the response to faces and the response to objects. Objects were also used as the comparison category to compute scene

selectivity and body selectivity. Object selectivity was defined as the difference between the response to objects and the response to scrambled objects.

The Variable-Window Method. To avoid both the subjectivity of manually setting thresholds and the problem of how to deal with data from participants who have responses below typically used thresholds, we adopted the "variable-window" method used in several recent papers (28, 29, 38, 39). We first made surface masks at the expected location for each ROI we planned to analyze. The mask was manually prepared by referring to the category-selective voxels of both groups at a liberal threshold ($P < 0.05$), so as to include all voxels that could be considered part of a particular category-selective area (see *SI Appendix*, Fig. S2 to view the masks). We then identified each participant's ROI by selecting the most selective voxels in the mask. To determine whether our results are consistent across different ROI sizes, we compared selectivity between DPs and controls at varied ROI sizes, ranging from 5 to 35% in 5% steps. This method provided a simple but effective way to balance the trade-off between extent and selectivity and ensured a fair comparison between controls and DPs.

Results

Normal Organization of Category-Selective Areas in DP. To compare the overall distribution of category-selective responses in the 22 DPs and 27 controls, a group-level analysis was performed for each category and each group of participants. In Fig. 1A, each of the category-selective significance maps shows the clusters that were more responsive to either faces, scenes, bodies, or objects than the contrast category. For all four contrasts, controls and DPs had similar category-selectivity maps. Clusters that were significantly face-selective appear in the fusiform gyrus, along the
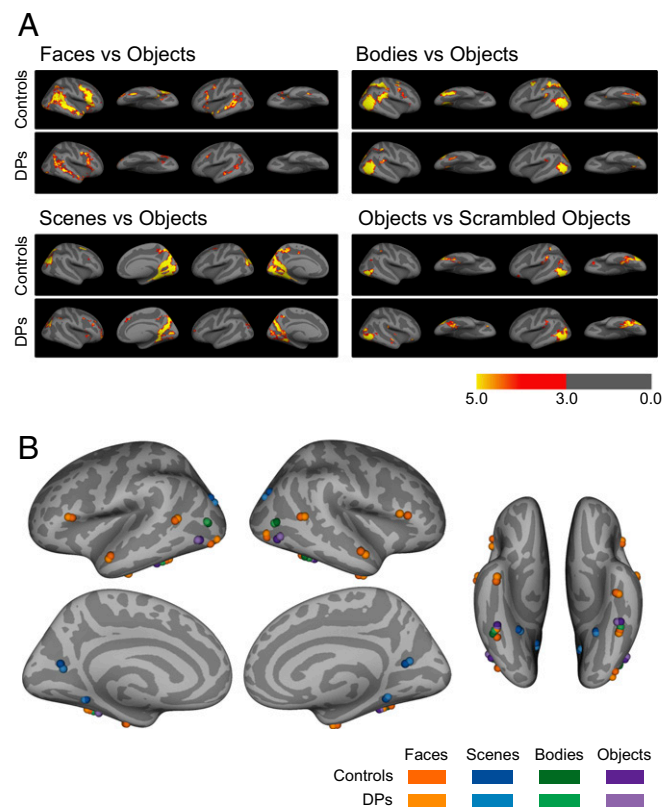
Fig. 1. Whole-brain organization of category-selective areas in DPs and controls. (A) The whole-brain significance maps for each visual category ($P < 0.001$, clusterwise-corrected). The location of selective areas in controls and DPs was similar for all categories, but the DPs had noticeably weaker activations and smaller cluster sizes for all categories except objects. (B) Group peak coordinates extracted for each functional ROI analyzed. Darker dots display peaks for the control group, and lighter dots represent peaks for the DPs. DPs and controls had very similar peak coordinates.

Jiahui et al.

superior temporal sulcus (STS), and in the frontal lobe. Scenes selectively activated areas spread from occipital cortex to medial parietal cortex and parahippocampal gyrus. Body-selective and object-selective areas were distributed mainly along the fusiform gyrus and occipital cortex. Except for object-selective areas, clusters in DPs were noticeably smaller and exhibited weaker significance than the same clusters in controls. The average peak coordinates for each ROI showed DPs and controls had extremely similar peak coordinates (Fig. 1B and *SI Appendix*, Table S1; see *SI Appendix* for how the peak coordinates were located). These comparisons indicate the general organization of visual recognition in DPs is comparable to that found in participants with normal face processing.

Widespread Deficits in Face-Processing System. Having compared the category-selective organization in DPs and controls, we next investigated the tuning profiles in the face-selective areas using the variable-window method. Before comparing category selectivity, we confirmed that controls and DPs had similar amounts of head motion in the scanner and that the functional signal-to-noise ratios of all ROIs were comparable for the two groups (see *SI Appendix, SI Analysis* for details).

We first report results from analyses using the 10% most face-selective voxels as the ROI, as was done in previous reports (28, 29, 38, 39). In four of the six face-selective ROIs in the right hemisphere, DPs had significantly weaker face selectivity than controls [Fig. 2A; fusiform face area (FFA): $t(45) = 2.96$, $P = 0.005$; posterior STS (pSTS): $t(45) = 3.48$, $P = 0.001$; anterior STS (aSTS): $t(45) = 3.29$, $P = 0.002$; inferior frontal gyrus (IFG): $t(45) = 2.78$, $P = 0.008$]. These reductions in selectivity were driven by reduced responses to faces, not increased responses to objects (Fig. 2B; Tukey test; FFA: face, $z = 3.93$, $P < 0.001$, object, $z = 0.63$, $P = 0.53$; pSTS: face, $z = 2.95$, $P = 0.003$, object, $z = -0.82$, $P = 0.41$; aSTS: face, $z = 4.04$, $P < 0.001$, object, $z = -0.27$, $P = 0.79$; IFG: face, $z = 2.53$, $P = 0.01$, object, $z = 0.62$, $P = 0.54$). Significance values of all four ROIs remained significant after correction with the Holm–Bonferroni method for multiple comparisons (40–42). DP face selectivity in the other two ROIs in the right hemisphere was also weaker than control selectivity, but these differences were not statistically significant [Fig. 2A; occipital face area (OFA): $t(45) = 1.10$, $P = 0.28$; anterior temporal lobe (ATL): $t(45) = 1.82$, $P = 0.08$].

DP face selectivity in all face ROIs in the left hemisphere was weaker than selectivity in controls, but only left FFA reached significance [Fig. 2A; $t(45) = 3.01$, $P = 0.005$; Holm–Bonferroni-corrected] while left OFA was marginally significant [Fig. 2A; $t(45) = 1.94$, $P = 0.06$]. As above, the selectivity reductions in these two regions resulted primarily from weaker responses to faces in DPs, not stronger responses to objects (Fig. 2B; FFA: face, $z = 2.89$, $P = 0.004$, object, $z = 0.37$, $P = 0.71$; OFA: face, $z = 2.20$, $P = 0.03$, object, $z = 0.97$, $P = 0.33$). None of the other face-selective ROIs in the left hemisphere reached significance for face selectivity [Fig. 2A; pSTS: $t(45) = 1.15$, $P = 0.25$; aSTS: $t(45) = 1.62$, $P = 0.11$; IFG: $t(45) = 1.57$, $P = 0.12$; ATL: $t(45) = 1.37$, $P = 0.18$].

We validated our parametric results by doing a bootstrap analysis with 10,000 repetitions. This nonparametric analysis generated the same results as described above (Holm–Bonferroni-corrected). Examination of individual DP's face selectivity suggested the group differences in face areas did not result from a subset of DPs with extremely low selectivity across many of the ROIs (*SI Appendix*, Figs. S10 and S11).

A 2 (anterior/posterior) × 2 (control/DP) × 6 (ROIs) ANOVA revealed comparable reductions in face selectivity in the anterior and posterior ROIs [*SI Appendix*, Fig. S3C; $F(1,45) = 1.47$, $P = 0.23$]. Results of the individual ROI analyses found significant differences in four right hemisphere areas but only one left hemisphere area, but a 2 (left/right) × 2 (control/DP) × 6 (ROIs) ANOVA did not reveal a significant right hemisphere bias [*SI*

Appendix, Fig. S3C; $F(1,45) = 1.80$, $P = 0.19$]. Similarly, a 2 (dorsal/ventral) × 2 (control/DP) × 6 (ROIs) ANOVA on the dorsal and ventral stream ROIs across hemispheres did not find a difference in the reduction of face selectivity between ROIs in the two streams [*SI Appendix*, Fig. S3C; $F(1,45) = 0.62$, $P = 0.43$].

To evaluate the consistency of our findings at different ROI sizes, we calculated face selectivity for ROIs of different sizes by changing the percentage of voxels selected (Fig. 2C). Each ROI included the top X% (range: 5–35) of voxels in each functional mask with the strongest response preference for faces over objects. As expected (28, 39), the magnitude of face selectivity dropped as the percentage increased, but the difference in face selectivity between DPs and controls at different percentages was similar to what was found at 10% across all ROIs (Fig. 2C and *SI Appendix*, Fig. S3B). Across the different percentages, selectivity differences were driven by reduced responses to faces in DPs and not increased responses to objects (*SI Appendix*, Fig. S3A).

Face-Selectivity Deficits Are Restricted to Face Network. The analyses above demonstrate the DPs had weaker face selectivity across the face network and that this reduction was driven by reduced responses to faces. Areas selective for scenes, bodies, and objects also show responses to faces (43), so we next examined whether DPs also show abnormal responses to faces in these areas. To answer this question, we analyzed commonly investigated scene-, body-, and object-selective ROIs (43–45) using a procedure similar to that used for the face-selective ROIs. In each functional mask covering the expected location of a category-selective area, the top 10% of voxels that were most scene-, body-, or object-selective were selected as ROIs. Face selectivity in each category-selective ROI was then calculated for both groups by contrasting the response to faces and objects. Because many of the masks for the nonface ROIs overlapped with face masks, they often contained a substantial number of face-selective voxels that were analyzed as part of the face ROIs discussed above. To make sure the results were not affected by those face-selective voxels, we carried out the analyses after removing face-selective voxels (see *SI Appendix, SI Analysis* for analysis details). Face selectivity in the DPs was not significantly reduced in any of the nonface ROIs [Fig. 3; ROI abbreviations are defined in the text (l indicates left and r indicates right); rPPA: $t(45) = -1.59$, $P = 0.12$; rOPA: $t(45) = -1.21$, $P = 0.23$; rMPA: $t(45) = -0.33$, $P = 0.74$; lPPA: $t(45) = -1.79$, $P = 0.08$; lOPA: $t(45) = -0.43$, $P = 0.67$; lMPA: $t(45) = -0.51$, $P = 0.61$; rEBA: $t(45) = 0.96$, $P = 0.34$; rFBA: $t(43) = -0.01$, $P = 0.99$; lEBA: $t(45) = 0.08$, $P = 0.93$; lFBA: $t(41) = 0.53$, $P = 0.60$; rLO: $t(45) = 0.83$, $P = 0.41$; rpFs: $t(45) = 0.35$, $P = 0.73$; lLO: $t(45) = -0.86$, $P = 0.39$; lpFs: $t(45) = 0.28$, $P = 0.78$]. Similarly, if the analyses included the removed voxels, none of the ROIs showed significant differences (*SI Appendix*, Fig. S4). These results indicate that DP face-selectivity deficits are limited to the face system and tentatively suggest their behavioral deficits with faces do not result from impairments in other category-selective regions.

Broad Deficits in Visual-Recognition Mechanisms. Little is known about the extent of the cortical abnormalities associated with DP, so we next compared selectivity to the preferred category in areas selective for scenes, bodies, and objects between DPs and controls.

Selectivity to scenes in scene-selective areas. In the scene-selective areas, we used the variable-window method to measure selectivity. Masks were created for three ROIs [parahippocampal place area (PPA), occipital place area (OPA), and medial place area (MPA)] in each hemisphere and the top 10% of the voxels that were most scene-selective based on the contrast of scenes > objects were analyzed. The ROI size was also varied in a later step from 5 to 35%.

In the right hemisphere, DP scene selectivity at the 10% level was significantly weaker than control selectivity in all three ROIs [Fig. 4A; PPA: $t(45) = 3.65$, $P < 0.001$; OPA: $t(45) = 2.02$,
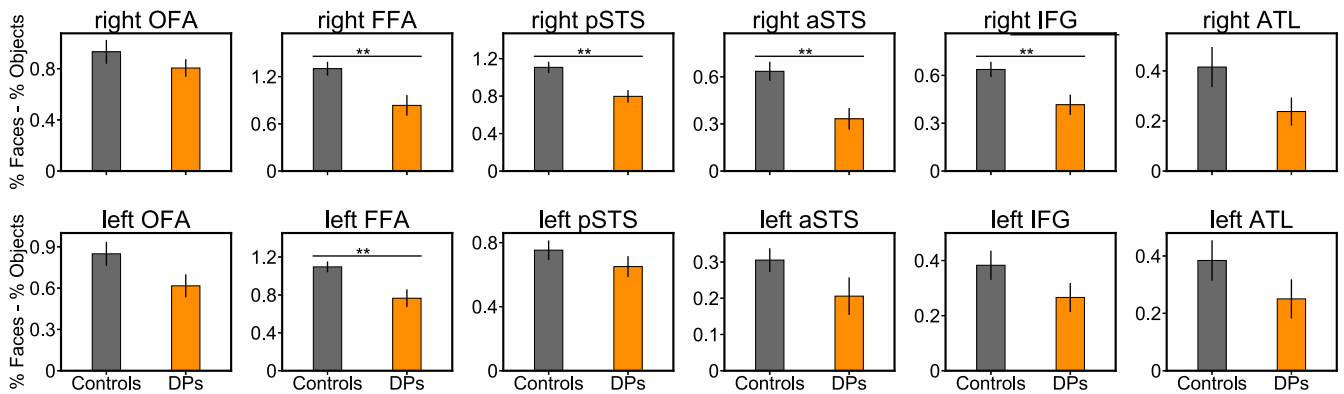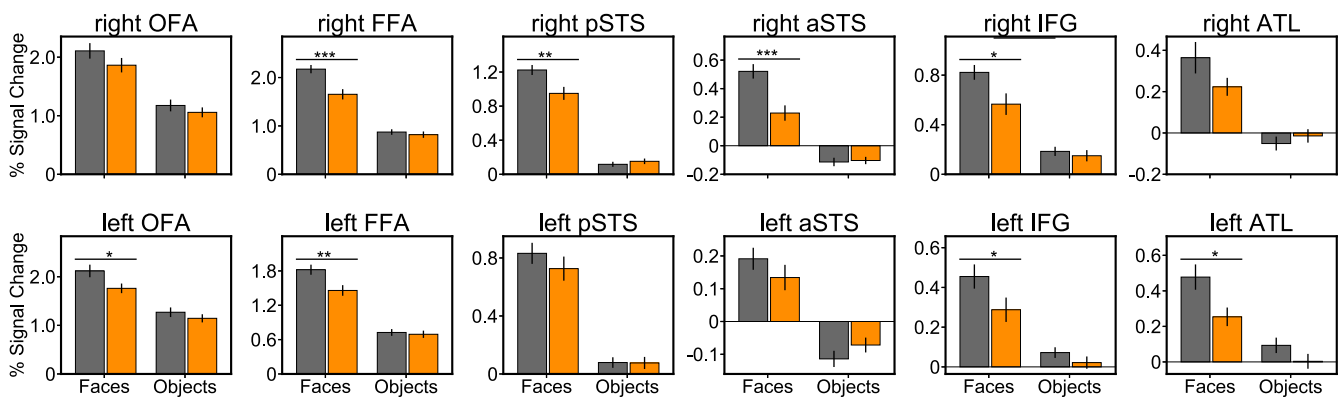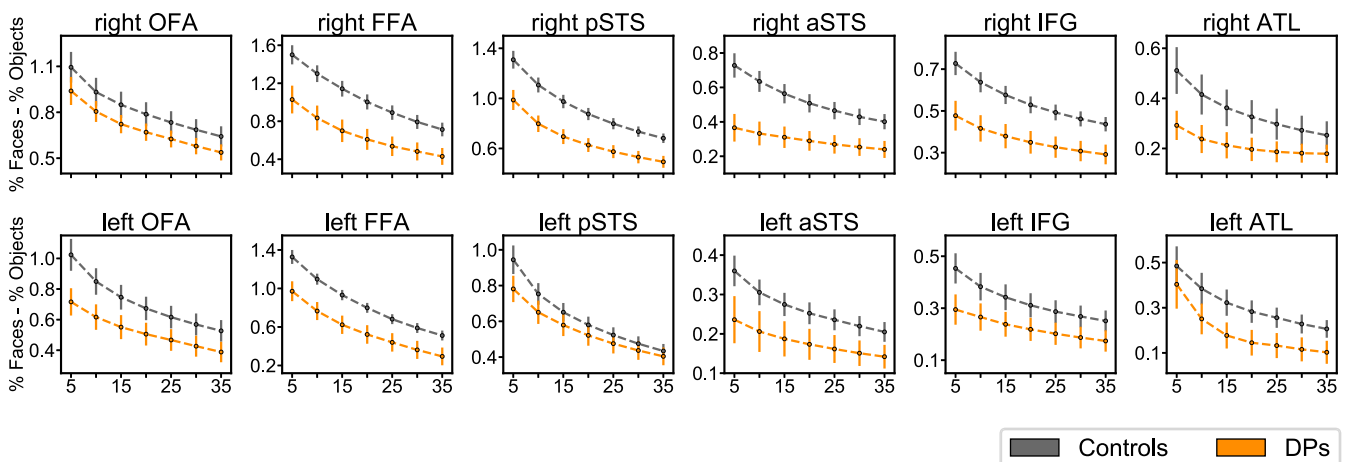
Fig. 2. DPs had widespread selectivity reductions in the face processing network. (*A*) Face selectivity and (*B*) responses to faces and objects in all face-selective ROIs at the 10% size. Significant reductions of face selectivity were found in four right-hemisphere ROIs and one left-hemisphere ROI, and the reductions in face selectivity were driven by weaker responses to faces. (*C*) Face selectivity at ROI sizes from 5 to 35%. The differences at 10% were comparable to results at other sizes. In all panels, error bars stand for ±1 SE for each group. ***$P < 0.001$, **$P < 0.01$, *$P < 0.05$.

$P = 0.05$; MPA: $t(45) = 3.73$, $P < 0.001$; all passed the Holm–Bonferroni correction]. The difference was driven primarily by weaker responses to scenes rather than increased responses to objects (Fig. 4*B*; Tukey test; PPA: scenes, $z = 2.75$, $P = 0.006$, objects, $z = 0.73$, $P = 0.47$; OPA: scenes, $z = 1.75$, $P = 0.08$,

objects, $z = 0.88$, $P = 0.38$; MPA: scenes, $z = 3.03$, $P = 0.002$, objects, $z = -0.09$, $P = 0.93$). In the left hemisphere, scene selectivity in the DPs was significantly reduced in PPA [Fig. 4*A*; $t(45) = 2.64$, $P = 0.01$, Holm–Bonferroni-corrected], reduced, though not significantly, in OPA [$t(45) = 1.12$, $P = 0.27$], and was
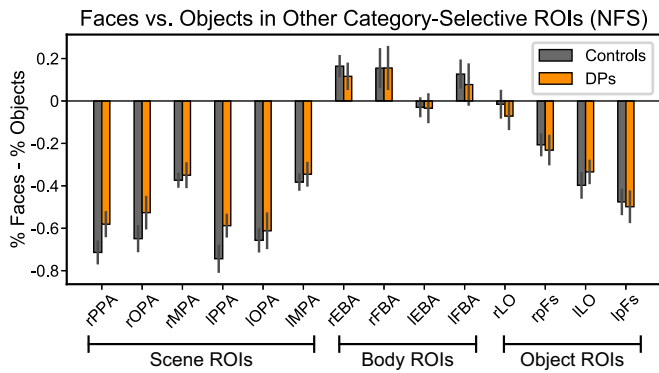
Fig. 3. Face selectivity in controls and DPs was comparable in ROIs outside the face network. Face selectivity in ROIs outside the face processing system when face-selective voxels ($P < 0.05$) were excluded from body ROIs (bilateral EBA and LO) and object ROIs (bilateral FBA and pFs). Face selectivity was comparable for controls and DPs across scene, body, and object ROIs. Error bars stand for ± 1 SE for each group. NFS, non-face-selective.

marginally significant in MPA [$t(45) = 1.96$, $P = 0.06$]. Bootstrap analysis revealed similar results (Holm–Bonferroni-corrected). In left PPA, we found a significant reduction in the response to scenes (Fig. 4B; Tukey test; scenes, z = 2.67, $P = 0.008$, objects, z = 1.16, $P = 0.25$). The reductions to scenes in left OPA

and left MPA were not significant (Tukey test; OPA: scenes, z = 0.10, $P = 0.92$, objects, z = −0.96, $P = 0.34$; MPA: scenes, z = 1.08, $P = 0.28$, objects, z = −0.65, $P = 0.52$). We did a 2 (left/right) × 2 (DP/control) × 3 (ROIs) ANOVA, which showed that group differences were more pronounced in the right hemisphere [$F(1,45) = 5.70$, $P = 0.02$].

Next, we varied the ROI percentage within each mask. The magnitude of selectivity decreased as ROI size increased, but the differences between the controls and DPs remained comparable (Fig. 4C and SI Appendix, Fig. S5 A and B).

Selectivity to human bodies in body-selective areas. Body-selective ROIs, based on bodies > objects contrasts, were examined with the variable-window method. Two ROIs in each hemisphere were included in the analysis: one on the lateral cortex (EBA) and the other on the fusiform gyrus (FBA). The difference in body selectivity between DPs and controls was marginally significant in EBA bilaterally [Fig. 5A; right EBA: $t(45) = 2.01$, $P = 0.05$; left EBA: $t(45) = 1.88$, $P = 0.07$]. Although the selectivity of bilateral FBA in the DPs was weaker than the selectivity in controls, the difference was not significant [Fig. 5A; right FBA: $t(45) = 1.48$, $P = 0.15$; left FBA: $t(45) = 0.26$, $P = 0.80$]. Bootstrap analysis generated similar results (Holm–Bonferroni-corrected). The response to bodies in the DPs was reduced relative to the controls, but none of the reductions reached significance (Fig. 5B; Tukey test; right EBA: body, z = 0.64, $P = 0.53$, object, z = −1.20, $P = 0.23$; right FBA: body, z = 1.26, $P = 0.21$, object, z = 0.05, $P = 0.96$; left EBA: body, z = 0.77, $P = 0.44$, object, z = −0.70, $P = 0.48$;

A   Scene Selectivity (10%)

B   Scenes & Objects (10%)

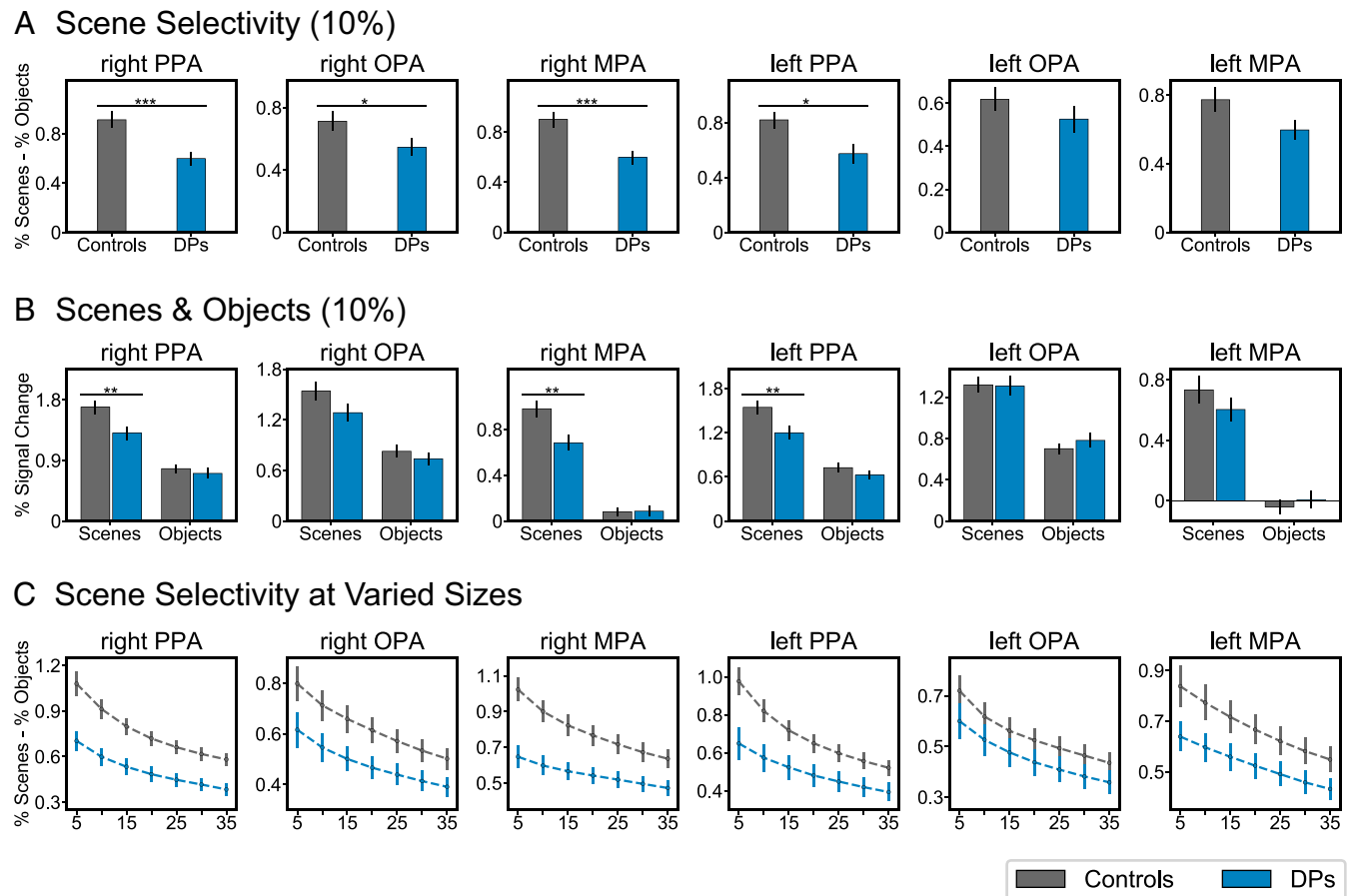## C   Scene Selectivity at Varied Sizes

Controls   DPs

Fig. 4. DPs had scene-selectivity reductions in scene-selective ROIs. (A) Scene selectivity and (B) responses to scenes and objects in all scene-selective ROIs at 10% size. Significant reductions of scene selectivity were found in all three right ROIs and one left ROI, and the reductions of scene selectivity were driven by weaker responses to scenes. (C) Scene selectivity at ROI sizes from 5 to 35%. The results at 10% were similar to those at other sizes. In all panels, error bars stand for ± 1 SE for each group. ***$P < 0.001$, **$P < 0.01$, *$P < 0.05$.

A Body Selectivity (10%)

B Bodies & Objects (10%)
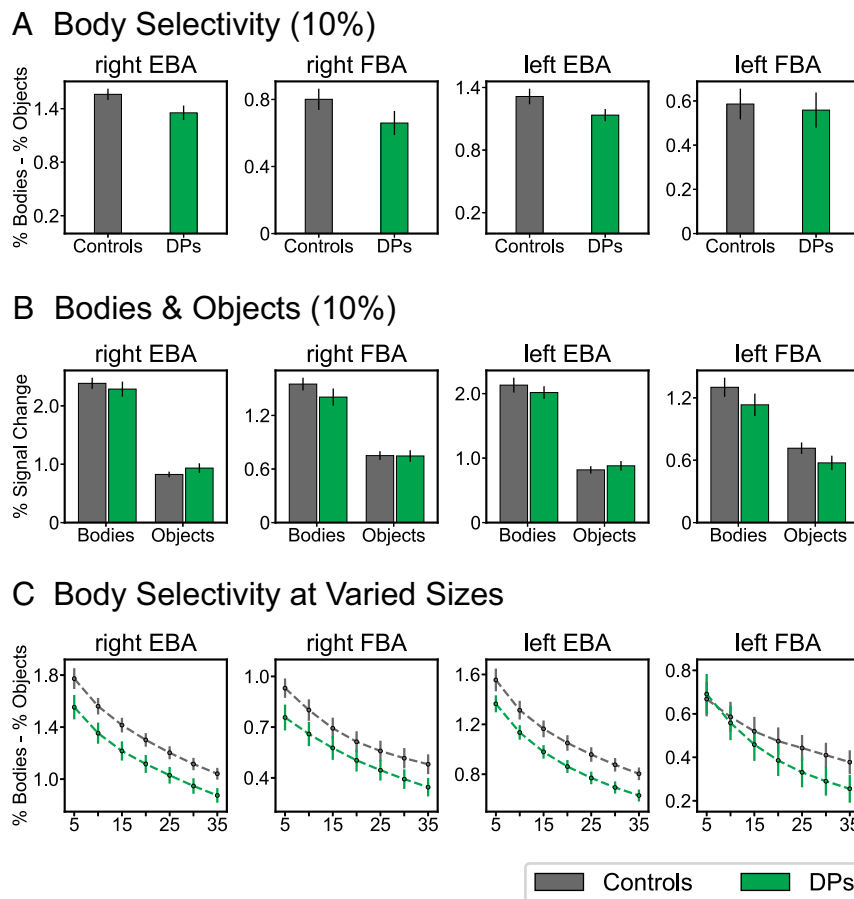

C Body Selectivity at Varied Sizes

Fig. 5. DPs had marginal body-selectivity reductions in body-selective ROIs. (*A*) Body selectivity and (*B*) responses to bodies and objects in all body-selective ROIs at 10%. Marginally significant reductions of body selectivity were found in right EBA (*P* = 0.05) and left EBA (*P* = 0.07). (*C*) This panel displays body selectivity at ROI sizes from 5 to 35%. The results at 10% were similar to the results at other sizes. In all panels, error bars stand for ±1 SE for each group.

left FBA: body, z = 1.23, *P* = 0.22, object, z = 1.64, *P* = 0.10). The results were similar at different ROI sizes (5–35%) (Fig. 5*C* and *SI Appendix*, Fig. S5 *C* and *D*).

Some voxels in EBA and FBA overlapped with face-selective ROIs so we excluded those voxels (*P* < 0.05 in face vs. object contrast) from the body-selective ROIs to prevent the face-selective voxels from contributing to group differences. The results were unchanged in either selectivity or in the responses to bodies (*SI Appendix*, Fig. S6).

Object selectivity in object-selective areas. Two object-selective ROIs [lateral occipital area (LO) and object-selective posterior fusiform area (pFs)] were localized in each hemisphere using the contrast of objects > scrambled objects. Unlike the other three category-selective contrasts, object selectivity in the DPs was similar to controls in all object-selective ROIs [Fig. 6*A*; right LO: *t*(45) = −0.38, *P* = 0.71; right pFs: *t*(45) = 0.14, *P* = 0.89; left LO: *t*(45) = 1.48, *P* = 0.15; left pFs: *t*(45) = −0.20, *P* = 0.84]. Bootstrap analysis also did not reveal any significant differences (Holm–Bonferroni-corrected). In all object-selective ROIs, DPs and controls showed comparable responses to objects and scrambled objects (Fig. 6*B*; Tukey test; right LO: objects, z = 0.24, *P* = 0.81, scrambled objects, z = 0.59, *P* = 0.56; right pFs: objects, z = −0.50, *P* = 0.62, scrambled objects, z = −0.53, *P* = 0.59; left LO: objects, z = 0.36, *P* = 0.72, scrambled objects, z = −0.87, *P* = 0.39; left pFs: objects, z = 0.71, *P* = 0.48, scrambled objects, z = 1.00, *P* = 0.32). The results were similar at different ROI sizes (*SI Appendix*, Fig. S7D). We again excluded the face-selective voxels (*P* < 0.05) from the object-

selective ROIs, and DPs and controls continued to show similar object selectivity and responses at all ROI percentages (*SI Appendix*, Fig. S7).

Selectivity reductions were limited to the preferred category in all ROIs. To examine whether selectivity differences to scenes and bodies were restricted to areas showing a preferential response to these categories, we separately tested for group differences in selectivity to scenes, bodies, and objects in the ROIs that showed selective responses to other categories. Scene selectivity was calculated in face-, body-, and object-selective ROIs. No significant group differences were discovered (*SI Appendix*, Fig. S8, Holm–Bonferroni-corrected). Similarly, for body and object selectivity, no significant differences between controls and DPs were seen in the ROIs that did not prefer those categories (*SI Appendix*, Fig. S8, Holm–Bonferroni-corrected). To exclude the effect of face-selective voxels in the body- and object-selective ROIs, those voxels were again excluded at *P* < 0.05 and the same analysis of group differences was then carried out. Again, no significant differences between the groups were found for the three categories in their nonpreferred ROIs (*SI Appendix*, Fig. S8, Holm–Bonferroni-corrected).

Discussion

Using the variable-window method, dynamic stimuli, and a relatively large sample size, our study was able to answer fundamental questions about the neural basis of DP and call attention to issues that will be important for future work. Comparison of the whole-brain distribution of category-selective areas and the peak
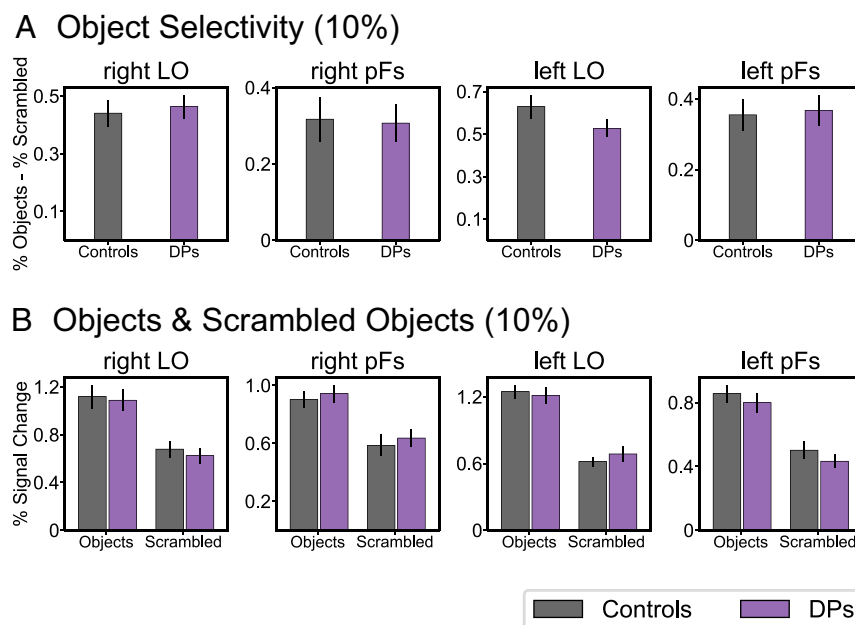
A Object Selectivity (10%)

B Objects & Scrambled Objects (10%)

Fig. 6. No deficits were found in object-selective ROIs. (*A*) Object selectivity and (*B*) responses to objects and scrambled objects in all object-selective ROIs at 10% size. No significant results were found in any ROIs. Figures displaying selectivity at different ROI percentages can be found in *SI Appendix*, Fig. S7D. In all panels, error bars stand for ±1 SE for each group.

voxel locations in DPs and controls (Fig. 1) indicated that visual recognition mechanisms in DP are organized normally (46), contrary to suggestions that individuals with selective developmental disorders have functional architectures that differ from neurotypical individuals (47, 48). Analyses of these ROIs, however, revealed that DPs have reduced selectivity for faces in face-selective areas and reduced selectivity for preferred categories in other category-selective areas.

Face Selectivity in DP. A leading neural account of DP proposes that it results from a disconnection between posterior face-selective areas (e.g., OFA and FFA) and ventral temporal anterior regions that process facial identity (9). While we found that DPs showed a nearly significant difference in face selectivity in the face ROI in the ventral anterior temporal lobe (ATL-FA), significant reductions in face selectivity were also present in right FFA, left FFA, and right pSTS-FA, contrary to what a disconnection hypothesis would predict. In addition, comparison of the selectivity differences between DPs and controls in anterior face ROIs (ATL-FA, aSTS-FA, and IFG-FA) vs. posterior face ROIs (OFA, FFA, and pSTS-FA) did not reveal a difference. Our results thus suggest that functional differences in posterior face-selective areas contribute to the face recognition deficits in DP. This conclusion is consistent with previous findings that also indicated abnormalities affecting or in the vicinity of posterior face areas (14–18, 20, 21) and with event-related potential studies that reported the N170, an early face-selective component generated by posterior face-selective areas (49, 50), responds atypically in a large proportion of DPs (51). Thus, our results support a distributed account rather than a disconnection account. The selectivity reductions we observed in some face ROIs may reflect the impact of reduced face selectivity in other face ROIs, but functional connectivity analyses will be necessary to better understand the interactions between face areas.

Our analyses of face selectivity in the face ROIs also allowed us to examine whether DPs showed differential reductions in ventral areas vs. dorsal areas. In the most prominent model of face processing (5, 52), ventral face areas are critical for the representation of invariant aspects of faces such as identity and sex whereas dorsal face areas represent changeable aspects of faces like expression and gaze. Many DPs perform normally with facial expression (53, 54) and eye gaze (55), so we expected selectivity in ventral areas would be more strongly reduced in DPs than selectivity in dorsal areas. However, selectivity in all three right hemisphere dorsal face areas was significantly weaker in DPs than in controls, and ventral-area selectivity was not more strongly reduced than dorsal-area selectivity. Previous DP imaging studies have tended to focus on ventral face areas, but dorsal, particularly STS, abnormalities have been reported as well (10, 14, 16, 56). The clear abnormalities we found in DP dorsal face areas raise questions about the computations carried out in these areas and suggest it would be valuable to carry out further testing of changeable aspects of face processing in DPs and to systematically examine DP performance with other STS-mediated abilities such as voice perception/recognition and biological motion perception (57).

Although pronounced reductions in face selectivity in face-selective ROIs were present in the DPs, we found no reductions in face selectivity in other category-selective areas. The restriction of face-selectivity reductions to face areas provides evidence that DPs' behavioral deficits with faces may result from problems limited to the face network. Nevertheless, the absence of group differences in non-face areas should be treated cautiously and further examined in future work. The normal response to faces in other category-selective areas also suggests the reductions found in face-selective areas are caused by deficient processing within the face network rather than reduced responses to faces in early visual areas, because problems originating in early visual areas would be expected to impact the response to faces in all category-selective ROIs.

DPs also Show Reduced Selectivity to Preferred Categories in Other Category-Selective Areas. Our study investigated the functioning of non-face category-selective areas ROIs in DP, and we found reductions in selectivity to the preferred category in a number of these ROIs. Selectivity to scenes in all scene-selective areas and to bodies in all body-selective areas was weaker in DPs than in controls. This weaker selectivity was significant in all three right-hemisphere scene-selective ROIs and one left-hemisphere

scene-selective ROI. For body-selective areas, two of the four ROIs were marginally significant. Similar to the findings in face-selective areas, these reductions were driven by weaker responses to the preferred category. As we found for face selectivity, scene-selectivity and body-selectivity reductions were restricted to the ROIs showing a preferential response to those categories. Surprisingly, the size of the group differences in two scene-selective ROIs (rMPA, rPPA) were comparable to the differences found in the face-selective ROIs exhibiting the largest group differences. It is possible that the use of bodies that were mostly covered by clothes may have underestimated the group differences in body-selective ROIs, because clothed bodies do not appear to fully engage body processing mechanisms (58).

Because selectivity in the DPs was weaker in all face, scene, and body areas, we considered several factors that might contribute to these differences. One possibility is that the DPs have impairments to early visual cortex so that category-selective areas receive insufficient input. However, deficits in upstream processes are unlikely to explain the reductions, because the responses to nonpreferred categories in DPs and controls were comparable (*SI Appendix*, Fig. S9). The group differences were also not the result of differences in head motion or functional signal-to-noise ratios (*SI Appendix, SI Methods*).

Are there other potential mechanisms that might cause the widespread selectivity deficits? One possibility concerns the nature of the information about the preferred category delivered to category-selective mechanisms. Normal participants show substantial variability in the location they initially fixate when viewing faces (59), and behavioral performance peaks when observers fixate faces at their preferred fixation location (60). It is possible that unlike normal participants, DPs do not preferentially fixate their optimal fixation location on the face. It is not known whether fixating away from one's optimal fixation location reduces neural responses to faces, but if it does, a mismatch between DPs' fixation locations and their optimal positions may contribute to the selectivity reductions in face ROIs. Another factor that may contribute to the selectivity reductions is the size of receptive fields in category-selective areas. A study with a small sample of DPs found that estimates of population receptive field size in posterior face-selective areas were smaller in DPs than in controls (61). Smaller receptive fields would be expected to reduce the quality of face input to face areas and lead to reduced responses. If DPs' receptive fields are small across a variety of category-selective areas, receptive field size may also account for weaker responses to scenes in scene areas and bodies in body areas.

The selectivity reductions found in non-face areas in the DPs may represent the neural correlates of behavioral deficits some DPs have with recognition tasks involving categories other than faces. These deficits include impairments with bodies (27, 53, 62), scenes (32), and objects (32, 33, 63, 64). Future studies can test this possibility by comparing selectivity in scene and body areas in DPs with normal scene and body recognition and DPs who have deficits with these categories. The common occurrence of object recognition deficits in DP (64) suggests the normal selectivity exhibited by the DPs in object-selective areas should be interpreted cautiously. It is worth noting that a number of DP cases with behavioral deficits limited to faces have been reported (32, 64–66), and the group differences we found in many of the non-face ROIs are not inconsistent with the presence of face-specific deficits in individual DPs. We expect that, similar to what is seen in acquired brain damage, face-selective cases of DP likely result from highly circumscribed cortical dysfunction whereas DPs with broad deficits have more extensive cortical dysfunction.

Developmental Factors Contributing to DP. Several findings suggest early face input is necessary for the face network to function

normally later in life (22, 23, 67). These findings have led to suggestions that DP may result from a lack of exposure to faces in childhood (24, 26, 68), but we are unaware of previous evidence that speaks to whether insufficient exposure to faces contributes to the emergence of DP. We believe, however, that the selectivity reductions in the DPs in scene-selective and body-selective areas indicate that inadequate experience with faces is unlikely to account for the face deficits in many of the participants tested here, because reduced face input would not be expected to lead to selectivity reductions in other category-selective areas. Restricted visual input during development might lead to reduced selectivity across many category-selective areas (69), but none of the DPs tested here had impaired scores on tests of low- and midlevel vision and none reported visual problems early in life.

The widespread neural deficits found in the DPs instead indicate DP often results from factors affecting the development of cortex well beyond face-selective areas. Many factors could be involved (e.g., neurotransmitter systems, myelination, pruning, etc.), and it seems likely that such factors would be unlikely to be limited to particular functional areas. Thus, these sorts of neurobiological factors would be expected to affect both face-selective areas and other category-selective areas in similar brain regions. Ramus has proposed an influential theory that developmental disorders such as DP, dyslexia (70), dyscalculia (71), and amusia (72) result from a particular neurobiological problem: neural migration errors. These errors lead to focal cortical disorganization, and according to this view, the type of behavioral deficit that results from the disorganization depends on the computations normally carried out in the affected cortex. For example, anomalies in left perisylvian cortex will tend to cause phonological deficits, whereas anomalies to face-selective areas of right fusiform gyrus might result in prosopagnosia. Autopsies of dyslexic brains found that cortical anomalies were concentrated in regions critical for speech and language but were also present in lower concentrations in neighboring regions (73–75). Further support for the role of neural migration in dyslexia comes from studies showing that the majority of genes associated with dyslexia play a role in neural migration (76). Ramus (70) has suggested this neural migration model of dyslexia may be applicable to DP, and the extensive selectivity reductions in the DPs tested here as well as the heritability of DP (33, 77–79) fit with his proposal. Looking ahead, the well-characterized functional organization of visual recognition provides a unique opportunity to assess the neural scope of a selective developmental disorder, and it will be informative to determine how often DPs have functional abnormalities in regions surrounding those examined here.

Summary and Future Directions

DPs exhibited reduced face selectivity across many face-selective ROIs, and these reductions were not concentrated within particular divisions of the face network. Selectivity reductions were also present for scenes and bodies in areas selective for those categories. These widespread selectivity reductions suggest face recognition deficits in a substantial proportion of DPs are only the most noticeable visual recognition deficit, and we hope the recognition of these broader abnormalities encourages visual neuropsychologists to widen the lens beyond DP to address the variety of developmental visual recognition disorders that occur.

1. Behrmann M, Scherf KS, Avidan G (2016) Neural mechanisms of face perception, their emergence over development, and their breakdown. *Wiley Interdiscip Rev Cogn Sci* 7: 247–263.
2. Susilo T, Duchaine B (2013) Advances in developmental prosopagnosia research. *Curr Opin Neurobiol* 23:423–429.
3. Dalrymple KA, et al. (2014) "A room full of strangers every day": The psychosocial impact of developmental prosopagnosia on children and their families. *J Psychosom Res* 77:144–150.
4. Yardley L, McDermott L, Pisarski S, Duchaine B, Nakayama K (2008) Psychosocial consequences of developmental prosopagnosia: A problem of recognition. *J Psychosom Res* 65:445–451.
5. Haxby JV, Hoffman EA, Gobbini MI (2000) The distributed human neural system for face perception. *Trends Cogn Sci* 4:223–233.
6. Grill-Spector K, Weiner KS (2014) The functional architecture of the ventral temporal cortex and its role in categorization. *Nat Rev Neurosci* 15:536–548.
7. Duchaine B, Yovel G (2015) A revised neural framework for face processing. *Annu Rev Vis Sci* 1:393–416.
8. Avidan G, Behrmann M (2009) Functional MRI reveals compromised neural integrity of the face processing network in congenital prosopagnosia. *Curr Biol* 19:1146–1150.
9. Avidan G, Behrmann M (2014) Impairment of the face processing network in congenital prosopagnosia. *Front Biosci (Elite Ed)* 6:236–257.
10. Avidan G, et al. (2014) Selective dissociation between core and extended regions of the face processing network in congenital prosopagnosia. *Cereb Cortex* 24: 1565–1578.
11. Avidan G, Hasson U, Malach R, Behrmann M (2005) Detailed exploration of face-related processing in congenital prosopagnosia: 2. Functional neuroimaging findings. *J Cogn Neurosci* 17:1150–1167.
12. Avidan G, Tanzer M, Behrmann M (2011) Impaired holistic processing in congenital prosopagnosia. *Neuropsychologia* 49:2541–2552.
13. Thomas C, et al. (2009) Reduced structural connectivity in ventral visual cortex in congenital prosopagnosia. *Nat Neurosci* 12:29–31.
14. Garrido L, et al. (2009) Voxel-based morphometry reveals reduced grey matter volume in the temporal cortex of developmental prosopagnosics. *Brain* 132: 3443–3455.
15. Dinkelacker V, et al. (2011) Congenital prosopagnosia: Multistage anatomical and functional deficits in face processing circuitry. *J Neurol* 258:770–782.
16. Furl N, Garrido L, Dolan R, Driver J, Duchaine B (2011) Fusiform gyrus face-selectivity reflects facial recognition ability. *J Cogn Neurosci* 23:1723–1740.
17. Lohse M, et al. (2016) Effective connectivity from early visual cortex to posterior occipitotemporal face areas supports face selectivity and predicts developmental prosopagnosia. *J Neurosci* 36:3821–3828.
18. Song Y, Zhu Q, Li J, Wang X, Liu J (2015) Typical and atypical development of functional connectivity in the face network. *J Neurosci* 35:14624–14635.
19. Zhao Y, et al. (2016) Altered spontaneous neural activity in the occipital face area reflects behavioral deficits in developmental prosopagnosia. *Neuropsychologia* 89: 344–355.
20. Gomez J, et al. (2015) Functionally defined white matter reveals segregated pathways in human ventral temporal cortex associated with category-specific processing. *Neuron* 85:216–227.
21. Song S, et al. (2015) Local but not long-range microstructural differences of the ventral temporal cortex in developmental prosopagnosia. *Neuropsychologia* 78: 195–206.
22. Arcaro MJ, Livingstone MS (2017) A hierarchical, retinotopic proto-organization of the primate visual system at birth. *eLife* 6:e26196.
23. Le Grand R, Mondloch CJ, Maurer D, Brent HP (2003) Expert face processing requires visual input to the right hemisphere during infancy. *Nat Neurosci* 6:1108–1112.
24. Behrmann M, Avidan G (2005) Congenital prosopagnosia: Face-blind from birth. *Trends Cogn Sci* 9:180–187.
25. Johnson MH (2005) Subcortical face processing. *Nat Rev Neurosci* 6:766–774.
26. Johnson MH, Dziurawiec S, Ellis H, Morton J (1991) Newborns' preferential tracking of face-like stimuli and its subsequent decline. *Cognition* 40:1–19.
27. Righart R, de Gelder B (2007) Impaired face and body perception in developmental prosopagnosia. *Proc Natl Acad Sci USA* 104:17234–17238.
28. Norman-Haignere SV, et al. (2016) Pitch-responsive cortical regions in congenital amusia. *J Neurosci* 36:2986–2994.
29. Norman-Haignere S, Kanwisher N, McDermott JH (2013) Cortical pitch regions in humans respond primarily to resolved harmonics and are located in specific tonotopic regions of anterior auditory cortex. *J Neurosci* 33:19451–19469.
30. Zhang J, Liu J, Xu Y (2015) Neural decoding reveals impaired face configural processing in the right fusiform face area of individuals with developmental prosopagnosia. *J Neurosci* 35:1539–1548.
31. Duchaine B, Nakayama K (2006) The Cambridge face memory test: Results for neurologically intact individuals and an investigation of its validity using inverted face stimuli and prosopagnosic participants. *Neuropsychologia* 44:576–585.
32. Duchaine B, Nakayama K (2005) Dissociations of face and object recognition in developmental prosopagnosia. *J Cogn Neurosci* 17:249–261.
33. Duchaine B, Germine L, Nakayama K (2007) Family resemblance: Ten family members with prosopagnosia and within-class object agnosia. *Cogn Neuropsychol* 24: 419–430.
34. Duchaine B, Yovel G, Nakayama K (2007) No global processing deficit in the Navon task in 14 developmental prosopagnosics. *Soc Cogn Affect Neurosci* 2:104–113.
35. Fox CJ, Iaria G, Barton JJS (2009) Defining the face processing network: Optimization of the functional localizer in fMRI. *Hum Brain Mapp* 30:1637–1651.

36. Pitcher D, Dilks DD, Saxe RR, Triantafyllou C, Kanwisher N (2011) Differential selectivity for dynamic versus static information in face-selective cortical regions. *Neuroimage* 56:2356–2363.
37. Kriegeskorte N, Simmons WK, Bellgowan PS, Baker CI (2009) Circular analysis in systems neuroscience: The dangers of double dipping. *Nat Neurosci* 12:535–540.
38. Isik L, Koldewyn K, Beeler D, Kanwisher N (2017) Perceiving social interactions in the posterior superior temporal sulcus. *Proc Natl Acad Sci USA* 114:E9145–E9152.
39. Saygin ZM, et al. (2016) Connectivity precedes function in the development of the visual word form area. *Nat Neurosci* 19:1250–1255.
40. Aickin M (1999) Other method for adjustment of multiple testing exists. *BMJ* 318: 127–128.
41. Proschan MA, Waclawiw MA (2000) Practical guidelines for multiplicity adjustment in clinical trials. *Control Clin Trials* 21:527–539.
42. Zhang J, Quan H, Ng J, Stepanavage ME (1997) Some statistical methods for multiple endpoints in clinical trials. *Control Clin Trials* 18:204–221.
43. Schwarzlose RF, Swisher JD, Dang S, Kanwisher N (2008) The distribution of category and location information across object-selective regions in human visual cortex. *Proc Natl Acad Sci USA* 105:4447–4452.
44. Julian JB, Keinath AT, Frazzetta G, Epstein RA (2018) Human entorhinal cortex represents visual space using a boundary-anchored grid. *Nat Neurosci* 21:191–194.
45. Silson EH, Steel AD, Baker CI (2016) Scene-selectivity and retinotopy in medial parietal cortex. *Front Hum Neurosci* 10:412.
46. Eimer M, Gosling A, Duchaine B (2012) Electrophysiological markers of covert face recognition in developmental prosopagnosia. *Brain* 135:542–554.
47. Karmiloff-Smith A (2009) Nativism versus neuroconstructivism: Rethinking the study of developmental disorders. *Dev Psychol* 45:56–63.
48. Thomas M, Karmiloff-Smith A (2002) Are developmental disorders like cases of adult brain damage? Implications from connectionist modelling. *Behav Brain Sci* 25: 727–750, discussion 750–787.
49. Dalrymple KA, et al. (2011) The anatomic basis of the right face-selective N170 IN acquired prosopagnosia: A combined ERP/fMRI study. *Neuropsychologia* 49:2553–2563.
50. Sadeh B, Zhdanov A, Podlipsky I, Hendler T, Yovel G (2008) The validity of the face-selective ERP N170 component during simultaneous recording with functional MRI. *Neuroimage* 42:778–786.
51. Towler J, Gosling A, Duchaine B, Eimer M (2012) The face-sensitive N170 component in developmental prosopagnosia. *Neuropsychologia* 50:3588–3599.
52. Haxby JV, Gobbini MI (2011) Distributed neural systems for face perception. *Oxford Handbook of Face Perception*, Oxford Library of Psychology (Oxford Univ Press, Oxford), pp 93–110.
53. Biotti F, Gray KLH, Cook R (2017) Impaired body perception in developmental prosopagnosia. *Cortex* 93:41–49.
54. Humphreys K, Avidan G, Behrmann M (2007) A detailed investigation of facial expression processing in congenital prosopagnosia as compared to acquired prosopagnosia. *Exp Brain Res* 176:356–373.
55. Duchaine B, Jenkins R, Germine L, Calder AJ (2009) Normal gaze discrimination and adaptation in seven prosopagnosics. *Neuropsychologia* 47:2029–2036.
56. Behrmann M, Avidan G, Gao F, Black S (2007) Structural imaging reveals anatomical alterations in inferotemporal cortex in congenital prosopagnosia. *Cereb Cortex* 17: 2354–2363.
57. Deen B, Koldewyn K, Kanwisher N, Saxe R (2015) Functional organization of social perception and cognition in the superior temporal sulcus. *Cereb Cortex* 25: 4596–4609.
58. Bonemei R, Costantino AI, Battistel I, Rivolta D (2018) The perception of (naked only) bodies and faceless heads relies on holistic processing: Evidence from the inversion effect. *Br J Psychol* 109:232–243.
59. Peterson MF, Lin J, Zaun I, Kanwisher N (2016) Individual differences in face-looking behavior generalize from the lab to the world. *J Vis* 16:12.
60. Peterson MF, Eckstein MP (2012) Looking just below the eyes is optimal across face recognition tasks. *Proc Natl Acad Sci USA* 109:E3314–E3323.
61. Witthoft N, et al. (2016) Reduced spatial integration in the ventral visual cortex underlies face recognition deficits in developmental prosopagnosia. *bioRxiv*:10.1101/051102. Preprint, posted April 29, 2016.
62. Rivolta D, Lawson RP, Palermo R (2017) More than just a problem with faces: Altered body perception in a group of congenital prosopagnosics. *Q J Exp Psychol (Hove)* 70: 276–286.
63. Behrmann M, Avidan G, Marotta JJ, Kimchi R (2005) Detailed exploration of face-related processing in congenital prosopagnosia: 1. Behavioral findings. *J Cogn Neurosci* 17:1130–1149.
64. Geskin J, Behrmann M (2018) Congenital prosopagnosia without object agnosia? A literature review. *Cogn Neuropsychol* 35:4–54.
65. Duchaine BC, Yovel G, Butterworth EJ, Nakayama K (2006) Prosopagnosia as an impairment to face-specific mechanisms: Elimination of the alternative hypotheses in a developmental case. *Cogn Neuropsychol* 23:714–747.
66. Shah P, Gaule A, Gaigg SB, Bird G, Cook R (2015) Probing short-term face memory in developmental prosopagnosia. *Cortex* 64:115–122.
67. Moulson MC, Westerlund A, Fox NA, Zeanah CH, Nelson CA (2009) The effects of early experience on face recognition: An event-related potential study of institutionalized children in Romania. *Child Dev* 80:1039–1056.
68. Dalrymple KA, Corrow S, Yonas A, Duchaine B (2012) Developmental prosopagnosia in childhood. *Cogn Neuropsychol* 29:393–418.
69. Hasson U, Harel M, Levy I, Malach R (2003) Large-scale mirror-symmetry organization of human occipito-temporal object areas. *Neuron* 37:1027–1041.
70. Ramus F (2004) Neurobiology of dyslexia: A reinterpretation of the data. *Trends Neurosci* 27:720–726.

71. Butterworth B, Varma S, Laurillard D (2011) Dyscalculia: From brain to education. *Science* 332:1049–1053.
72. Peretz I (2016) Neurobiology of congenital amusia. *Trends Cogn Sci* 20:857–867.
73. Galaburda AM, Kemper TL (1979) Cytoarchitectonic abnormalities in developmental dyslexia: A case study. *Ann Neurol* 6:94–100.
74. Galaburda AM, Sherman GF, Rosen GD, Aboitiz F, Geschwind N (1985) Developmental dyslexia: Four consecutive patients with cortical anomalies. *Ann Neurol* 18:222–233.
75. Humphreys P, Kaufmann WE, Galaburda AM (1990) Developmental dyslexia in women: Neuropathological findings in three patients. *Ann Neurol* 28:727–738.
76. Carrion-Castillo A, Franke B, Fisher SE (2013) Molecular genetics of dyslexia: An overview. *Dyslexia* 19:214–240.
77. De Haan EH (1999) A familial factor in the development of face recognition deficits. *J Clin Exp Neuropsychol* 21:312–315.
78. Lee Y, Duchaine B, Wilson HR, Nakayama K (2010) Three cases of developmental prosopagnosia from one family: Detailed neuropsychological and psychophysical investigation of face processing. *Cortex* 46:949–964.
79. Schmalzl L, Palermo R, Coltheart M (2008) Cognitive heterogeneity in genetically based prosopagnosia: A family study. *J Neuropsychol* 2:99–117.

Supplementary Information for

Developmental Prosopagnosics Have Widespread Selectivity Reductions
Across Category-Selective Visual Cortex

Guo Jiahui, Hua Yang, and Bradley Duchaine

Guo Jiahui
Email: Jiahui.Guo.GR@dartmouth.edu

This PDF file includes:

Supplementary text
Figs. S1 to S11
Tables S1 to S2
References for SI reference citations

Supplementary Information Text

SI Experimental Procedures

SI Methods

Data Acquisition. All participants were scanned in a 3.0T Phillips MR scanner (Philips Medical Systems, WA, USA) with a SENSE (SENSitivity Encoding) 32-channel head coil. A high-resolution anatomical volume was acquired at the beginning of the scan using a high-resolution 3D magnetization-prepared rapid gradient-echo sequence (220 slices, field of view = 240 mm, acquisition matrix = 256×256, voxel size = $1 \times 0.94 \times 0.94$ mm). Functional images were collected using echo-planar functional images (time to repeat = 2000 ms, time echo = 35 ms, flip angle = 90°, voxel size = $3 \times 3 \times 3$ mm). Each volume consisted of 36 interleaved 3 mm thick slices with 0 mm interslice gap. We adopted oblique slice orientation aligned with each participant's anterior commissure–posterior commissure (AC–PC) line, because it produces fewer susceptibility artifacts than the commonly used transverse orientation (1) while also providing better coverage of the brain. The phase-encoding direction (anterior–posterior) was chosen to move the signal loss away from the more anterior part of the brain.

Data Preprocessing and Analysis. Data preprocessing and analysis were done using Freesurfer (https://surfer.nmr.mgh.harvard.edu/). Functional volumes were motion corrected and aligned to the anatomical volume for each participant. The aligned volume of each participant was resampled to the high-density surface mesh provided by Freesurfer, and then aligned to the standardized mesh of the template MNI305 FsAverage brain. The aligned functional volume was smoothed with a 4 mm FWHM (full width at half maximum) Gaussian kernel before analysis. Each voxel was fit with a general linear model (GLM) with one regressor per stimulus condition and the regressors for each stimuli condition were computed by modeling the hemodynamic response function (HRF). Following standard denoising procedures (2, 3), a linear-trend regressor and the first ten principal components from voxel responses in white matter were included to regress out signal drift and sources of noise with high variance across voxels as nuisance regressors in the model.

Whole-Brain Analysis. To produce the whole-brain group contrast maps in Fig. 1, voxels that were selectively activated by a particular category (e.g., faces > objects) were localized for each participant with all five runs. The individual contrast maps were then averaged across each group (controls and DPs). To correct for the multiple comparisons, the group selectivity map was corrected with Monte Carlo simulation at the voxel-wise threshold of p < 0.001 across the entire

brain surface (4). The voxel that showed the largest z-score in the contrast map to the preferred category (i.e., faces) was located with each ROI mask (described below), and this MNI coordinate was averaged across all five combinations (described below) to provide a stable and accurate estimate of the peak coordinate. Coordinates were averaged across participants in each group for each ROI investigated.

Removing Face-Selective Voxels from Non-Face ROIs. To get a cleaner measure of category-selectivity in the non-face ROIs that contain a substantial number of face-selective voxels, we deleted those voxels that were face-selective using a liberal threshold ($p < 0.05$) during the voxel selection procedure and then measured the category selectivity of the remaining voxels.

SI Analysis

Comparable Head Motion Between Controls and DPs. Did the DPs show weaker selectivity because their data was reduced in quality compared to the controls' data? Because the responses to the non-preferred categories were almost always comparable in DPs and controls (See Fig. S9), this possibility seems unlikely, but to directly address it, we compared DP and control head motion.

Framewise displacement (5) was calculated for each participant averaged across five runs. Comparison of mean brain displacement for the two groups was not significant ($t(45) = 0.43$, $p = 0.46$). Although one DP had more head motion than any other participant, the absolute amount of head motion was acceptable (0.31), and his selectivity was typical for the DP group. To take a closer look, we split the averaged brain displacement to check the amount of head motion in the single runs. We found an effect of run order ($F(4, 180) = 9.30$, $p < 0.001$), with more head motion in later runs. However, no significant differences were found between the groups ($F(1,45) = 0.20$, $p = 0.66$) or in the interaction between groups and runs ($F(4, 180) = 0.35$, $p = 0.84$). Controls and DPs were comparable in all five runs (Tukey test, all $p > 0.05$).

Comparable fSNR for Controls and DPs in All ROIs. Next we examined whether reduced fSNR in DPs may have contributed to their reduced selectivity. fSNR was defined as the offset of the regression model divided by the standard deviation of the residuals after removing task signal and nuisance regressors, and it was calculated for the averaged fSNR of each participant in each ROI. For each ROI, no significant difference was found between DPs and controls at the 10% level (all $p > 0.05$). In addition, no differences were present at other ROI percentages (5%-35%).
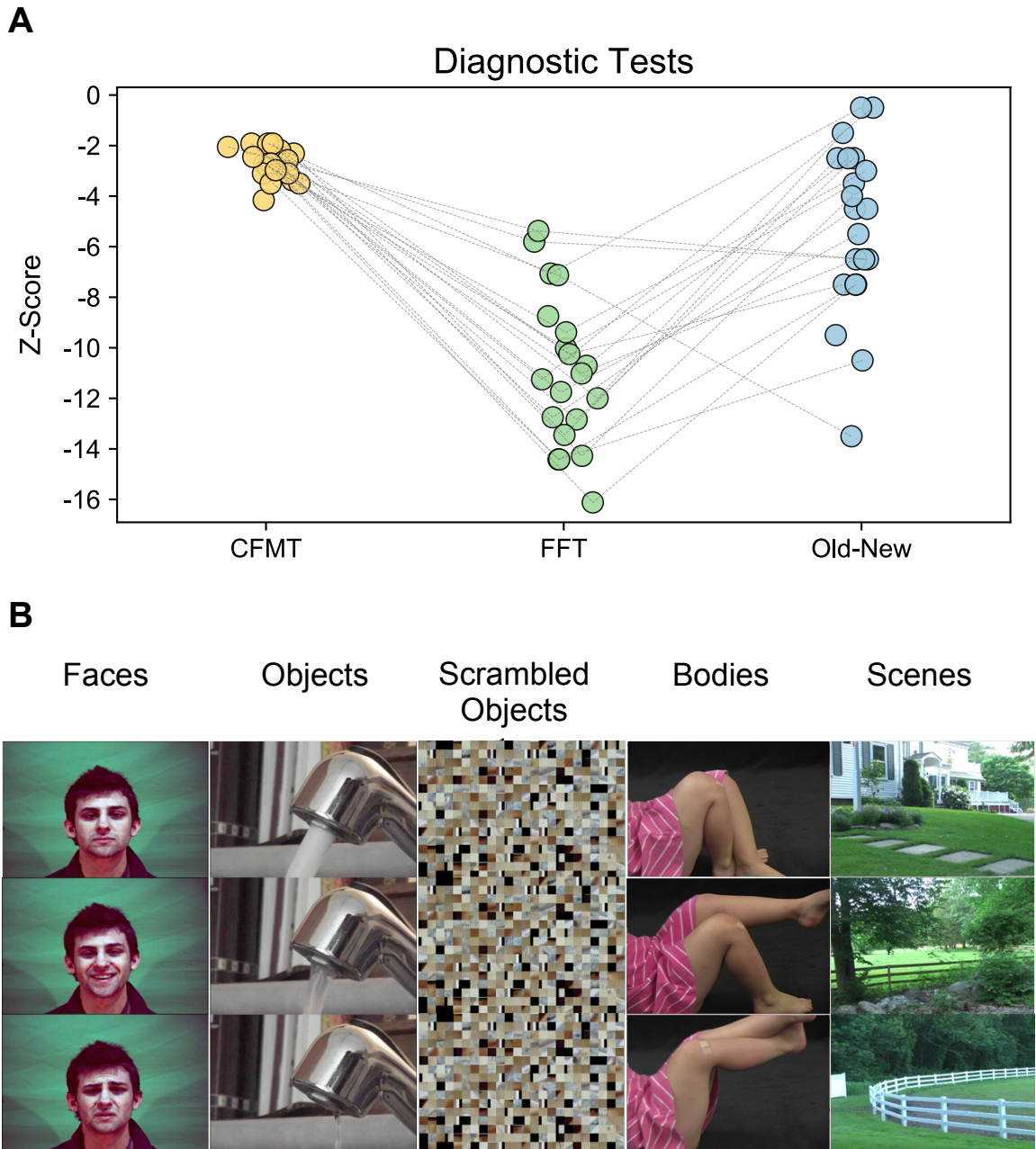
Fig. S1. DP performance on the diagnostic behavioral tests and example stimuli from the dynamic localizer. (A) DP were tested with the Cambridge Face Memory Test (CFMT), a famous face test (FFT), and an old-new face memory test. The DPs' scores were compared with 20 controls for the CFMT (mean age = 45.1 years) (6), 16 controls for the FFT (mean age = 39.3) (7), and 21 controls for the old-new test (mean age = 46.5) (7). Grey lines in the figure connects the three scores for each DP individual. **(B)** The dynamic localizer contains five categories, and each category was made up of a set of multiple short videos. This figure displays three frames from an example video for each category.
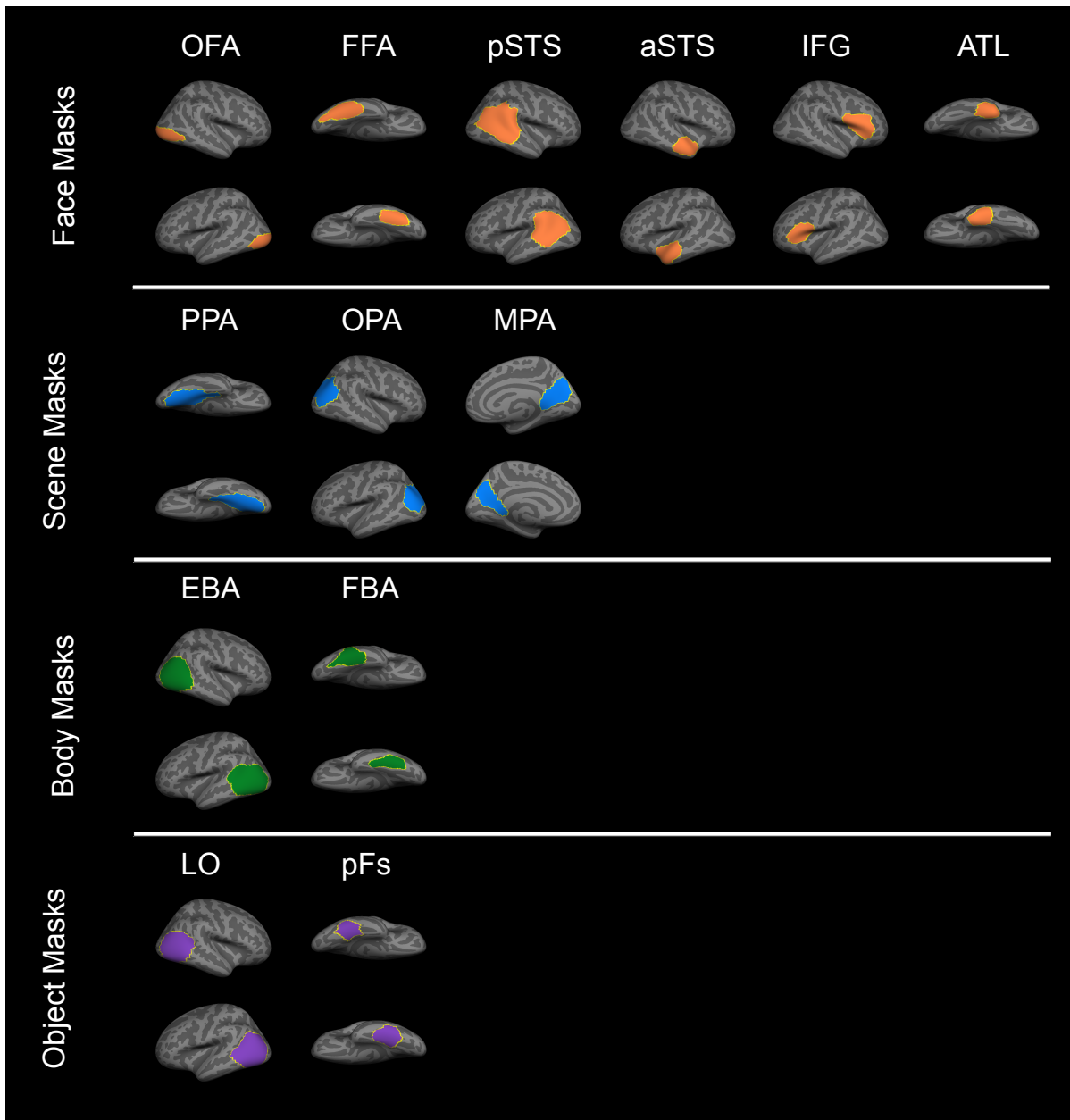
Fig. S2. Masks for each functional ROI. This figure shows the masks used for each category-selective ROI. Masks for face-selective areas are orange, scene-selective areas are blue, body-selective areas are green, and object-selective areas are purple. Masks for a category do not overlap with other masks for the same category.
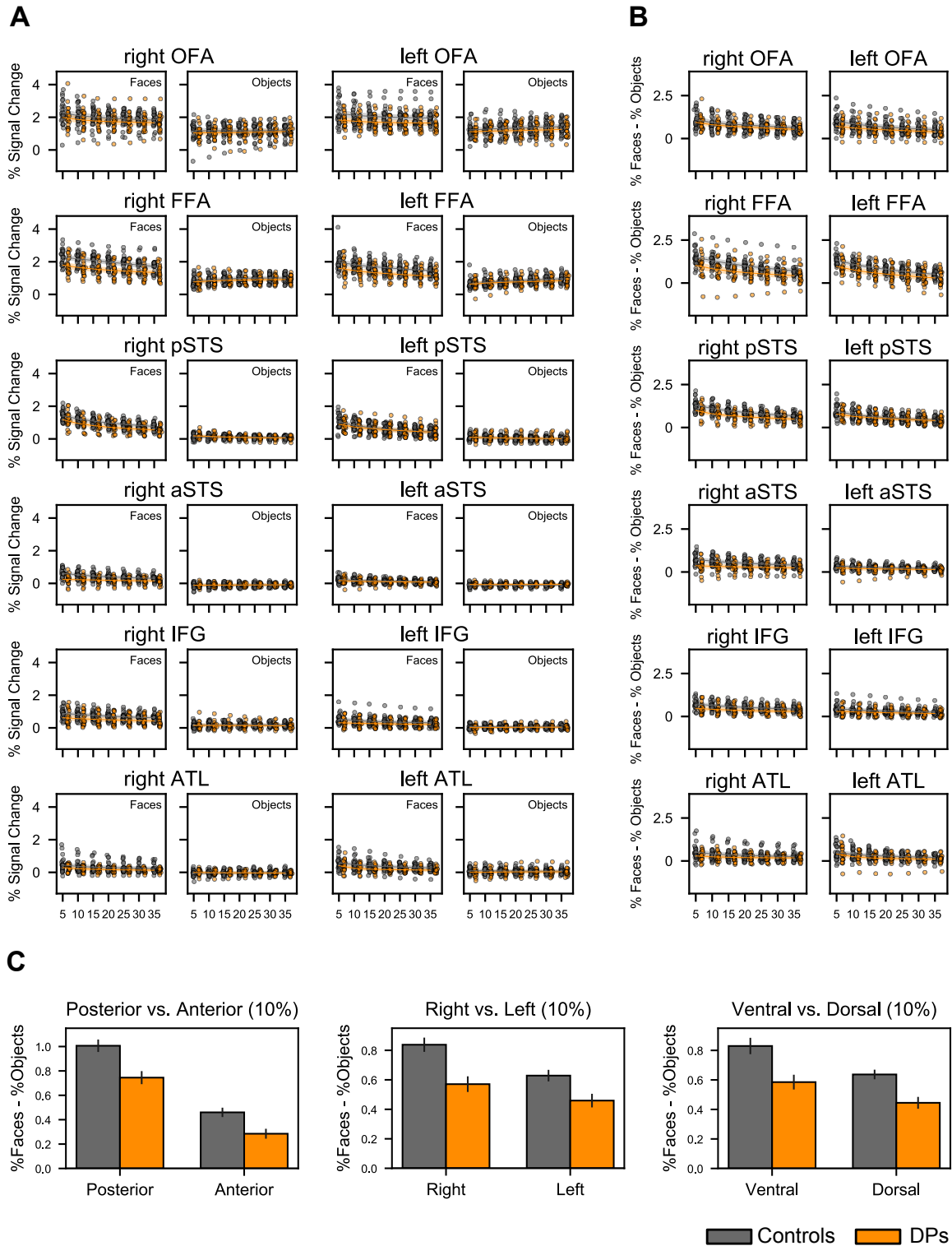
Fig. S3. Individual data for face selectivity and percent signal change to faces and objects in face ROIs, and controls' and DPs' face selectivity in posterior & anterior ROIs, in right &

left hemisphere ROIs, and in ventral & dorsal ROIs. (A) Individual data points for percent signal change to faces (left panels) and objects (right panels) at ROI sizes from 5% to 35%. **(B)** Individual data for face selectivity. In plots in **(A)** and **(B)**, the lines are the mean of each group, shaded areas above and below the line indicates ±1 standard error for each group. **(C)** Because no three-way interactions were found after including ROIs as a factor in the ANOVA (posterior/anterior x groups x ROIs: $F(5, 225) = 1.22$, $p = 0.30$; right/left x groups x ROIs: $F(5, 225) = 1.40$, $p = 0.23$; ventral/dorsal x groups x ROIs: $F(5, 225) = 1.96$, $p = 0.09$), we averaged posterior/anterior, right/left, or ventral/dorsal ROIs to plot this figure. The posterior vs. anterior panel demonstrates that the face-selectivity reductions in the DPs were comparable in posterior and anterior ROIs (2 (control/DP) x 2 (posterior/anterior) ANOVA: $F(1,45) = 1.47$, $p = 0.23$; Tukey Test: posterior, $z = 3.53$, $p < 0.001$; anterior, $z = 3.14$, $p = 0.002$). The right vs. left panel shows the face-selectivity reductions in the DPs were comparable in right and left hemisphere ROIs (2 (control/DP) x 2 (right/left) ANOVA: $F(1,45) = 1.80$, $p = 0.19$; Tukey Test: right, $z = 3.74$, $p < 0.001$; left, $z = 2.82$, $p = 0.005$). The ventral vs. dorsal panel shows that the DPs' face-selectivity reductions were comparable in ventral and dorsal ROIs (2 (control/DP) x 2 (ventral/dorsal) ANOVA: $F(1,45) = 0.62$, $p = 0.43$; Tukey Test: ventral, $z = 3.24$, $p = 0.001$; dorsal, $z = 3.76$, $p < 0.001$). In plots in **(C)**, error bars stand for ±1 standard error for each group. For all panels in Fig. S3, control group is gray, and DP group is orange. *** $p < 0.001$; ** $p < 0.01$.
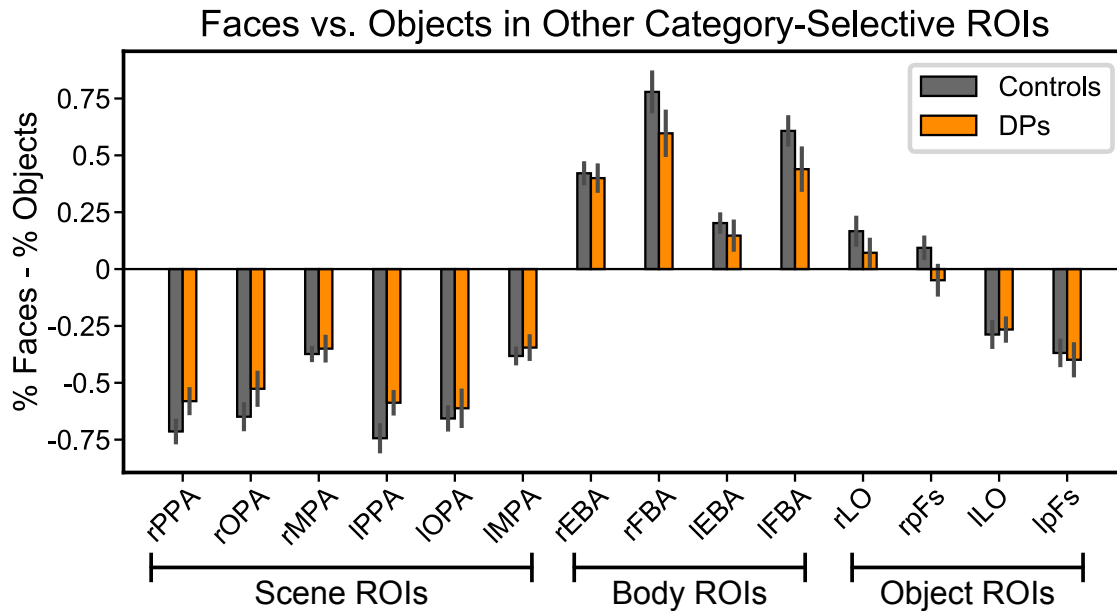
Fig. S4. Face selectivity in controls and DPs was also comparable in ROIs outside the face network when face-selective voxels are not excluded. This figure shows face selectivity in ROIs outside the face processing system when all voxels were included in body ROIs (bilateral EBA and LO) and object ROIs (bilateral FBA and pFs). Face selectivity was comparable for controls and DPs across scene, body, and object ROIs (rPPA: t(45) = -1.59, p = 0.12; rOPA: t(45) = -1.21, p = 0.23; rMPA: t(45) = -0.33, p = 0.74; lPPA: t(45) = -1.79, p = 0.08; lOPA: t(45) = -0.43, p = 0.67; lMPA: t(45) = -0.51, p = 0.61; rEBA: t(45) = 0.26, p = 0.80; rFBA: t(45) = 1.30, p = 0.20; lEBA: t(45) = 0.65, p = 0.52; lFBA: t(45) = 1.38, p = 0.17; rLO: t(45) = 1.00, p = 0.32; rpFs: t(45) = 1.58, p = 0.12; lLO: t(45) = -0.26, p = 0.80; lpFs: t(45) = 0.30, p = 0.76). Error bars stand for ±1 standard error for each group. PPA: parahippocampal place area; OPA: occipital place area; MPA: medial place area; EBA: extrastriate body area; FBA: fusiform body area; LO: lateral occipital area; pFs: object-selective posterior fusiform area.
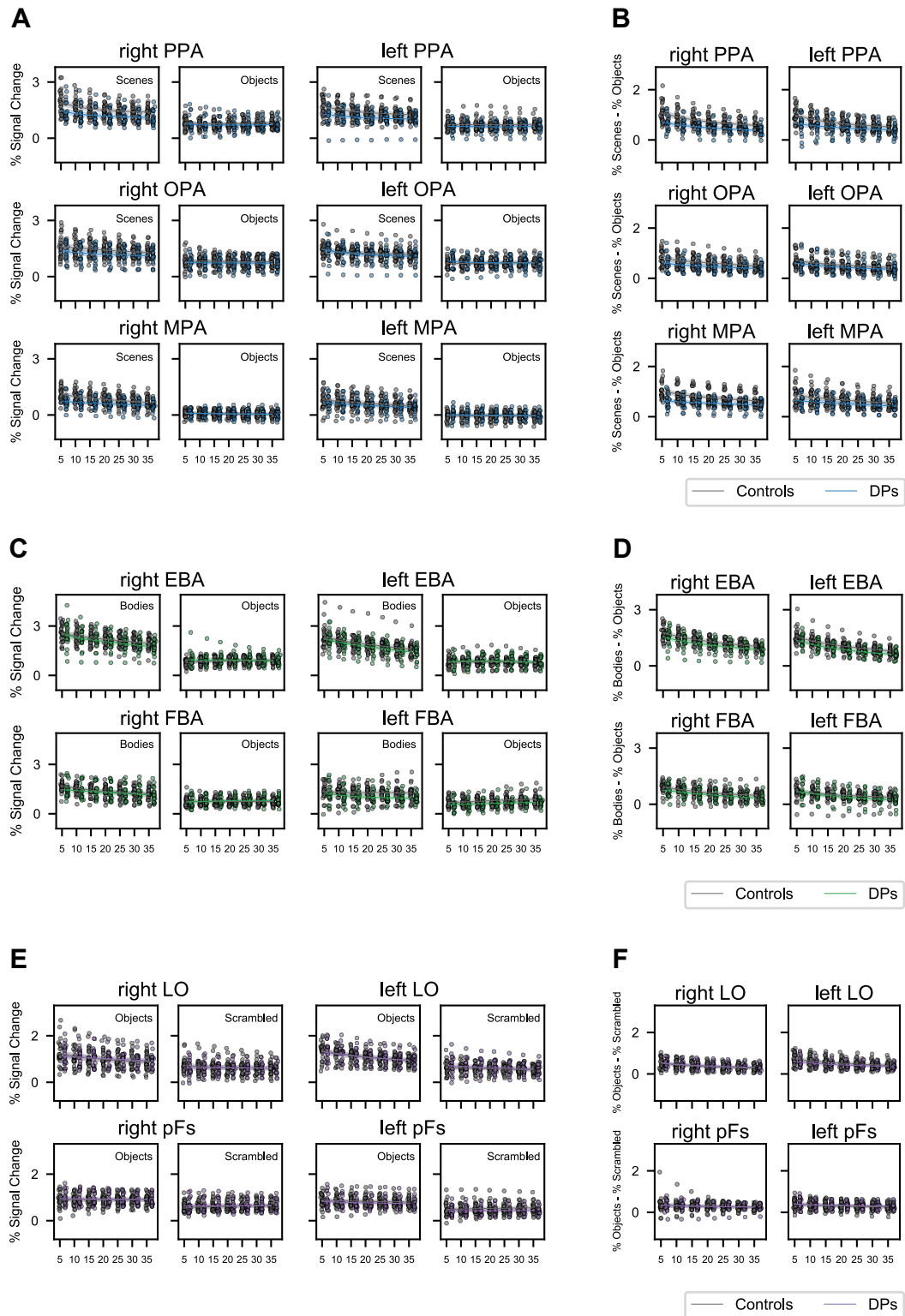
Fig. S5. Individual data for scene, body, and object ROIs. (A) Individual percent signal change to scenes (left panels) and objects (right panels) at ROI sizes from 5% to 35%. **(B)** Individual scene-

selectivity data. Control data points are gray, and DP data points are blue. **(C)** Individual percent signal change data to bodies (left panels) and objects (right panels) at ROI sizes from 5% to 35%. **(D)** Individual body-selectivity data. Control data is displayed in gray while DP data is green. **(E)** Individual percent signal change data to objects (left panels) and scrambled objects (right panels) both at ROI sizes from 5% to 35%. **(F)** Individual data for object selectivity. Controls are shown in gray and DPs in purple. In all panels, the lines are the mean of each group while the shaded areas above and below the line show ±1 standard error for each group.
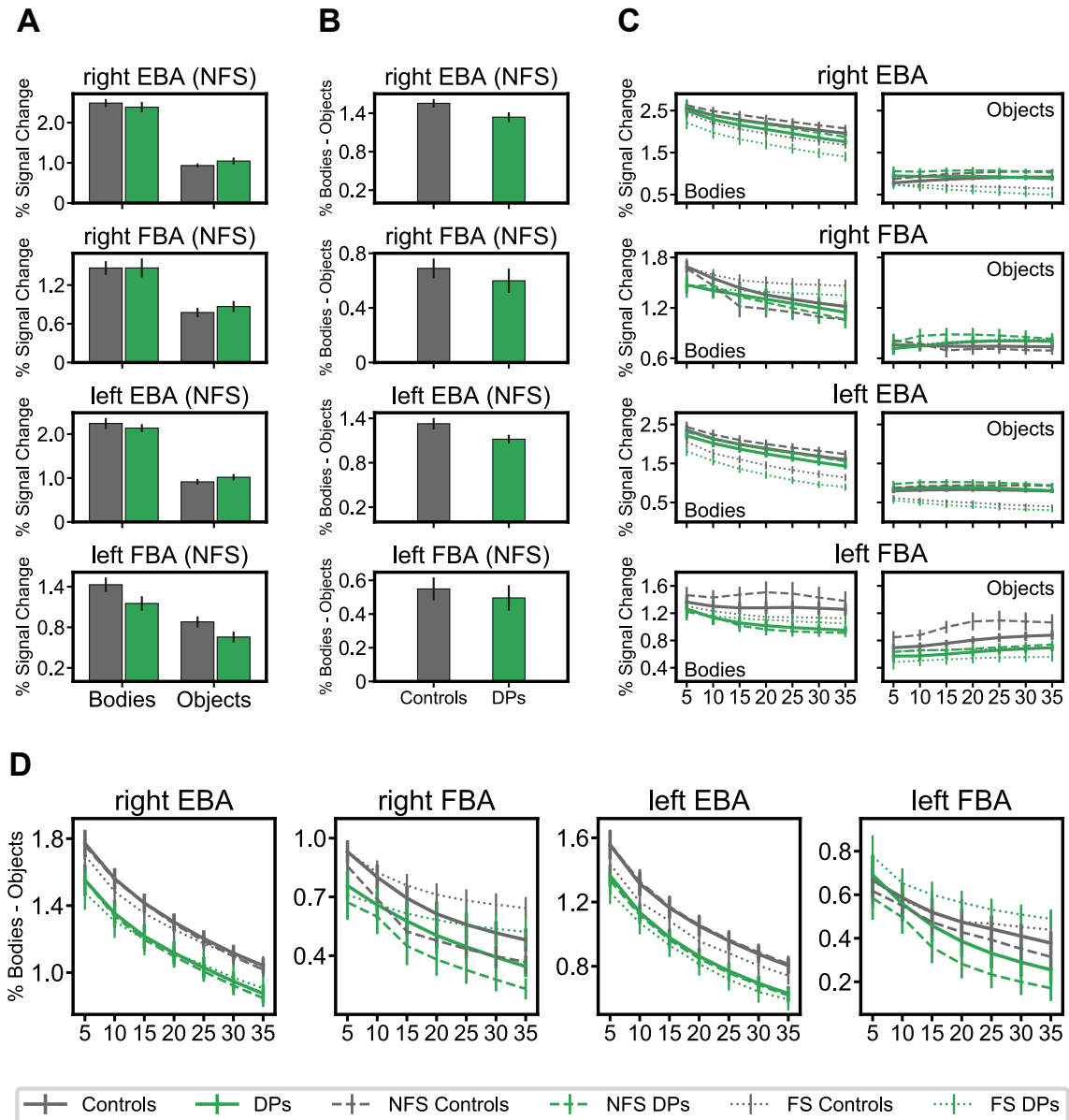
Fig. S6. Responses to bodies and objects after removing face-selective voxels. (A) and **(B)** show the responses to bodies and objects, as well as body-selectivity at 10% size after removing face-selective voxels ($p < 0.05$). **(C)** and **(D)** show the responses to bodies and objects, as well as body-selectivity at varied sizes in all three sets of voxels: all voxels included, face-selective voxels removed ($p >= 0.05$) (NFS), and only in the face-selective voxels ($p < 0.05$) (FS). NFS: Non-face-selective; FS: Face-selective. NFS lines largely overlap with the original lines with all voxels included in **(C)** and **(D)**, which indicates responses to bodies and objects as well as body selectivity tended to be similar after face-selective voxels were removed.
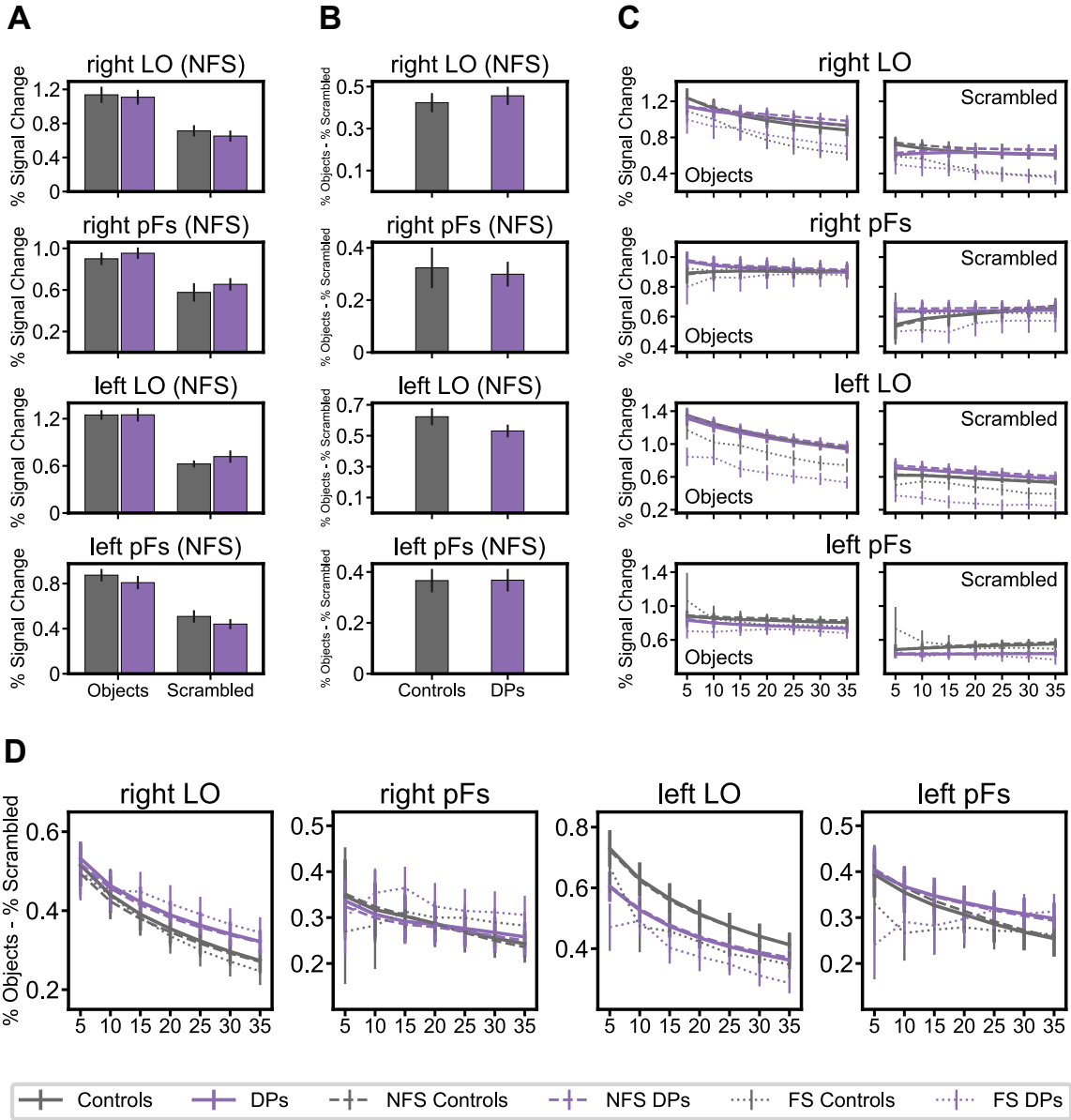
Fig. S7. Responses to objects and scrambled objects in object-selective areas after removing face-selective voxels. (A) and **(B)** show the responses to objects and scrambled objects, as well as object-selectivity at 10% size after removing face-selective voxels (p < 0.05). **(C)** and **(D)** show the responses to objects and scrambled objects, as well as object-selectivity at varied sizes in all three sets of voxels: all voxels included, face-selective voxels removed (p >= 0.05) (NFS), and only in the face-selective voxels (p < 0.05) (FS). NFS: Non-face-selective; FS: Face-selective. NFS lines largely overlap with the original lines with all voxels included in **(C)** and **(D)**, which indicates responses to objects and scrambled objects as well as object selectivity were generally similar after face-selective voxels were removed.
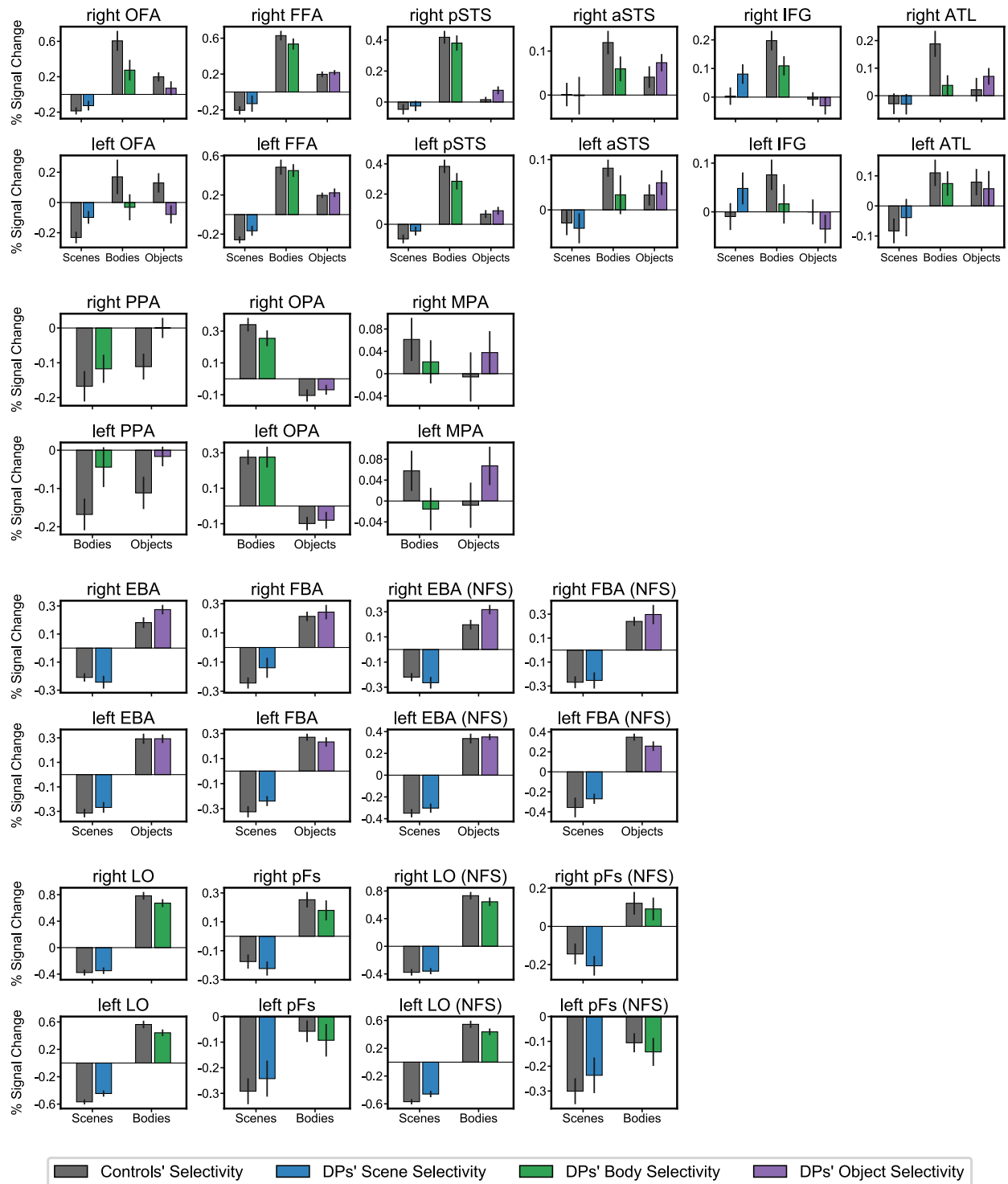
Fig. S8. Normal selectivity to non-preferred categories in scene, body, and object ROIs. Top two rows show scene, body, and object selectivity in face-selective ROIs; the 3rd and 4th rows show body and object selectivity in scene-selective ROIs; the 5th and 6th rows show scene and

object selectivity in body-selective ROIs; the last two rows show scene and body selectivity in object-selective ROIs. The selectivity of the DPs and controls was comparable for all categories in all ROIs (Holm-Bonferroni corrected), which demonstrates that reductions were limited to areas that show preferential responses to the category of interest. In all panels, error bars stand for ±1 standard error for each group.
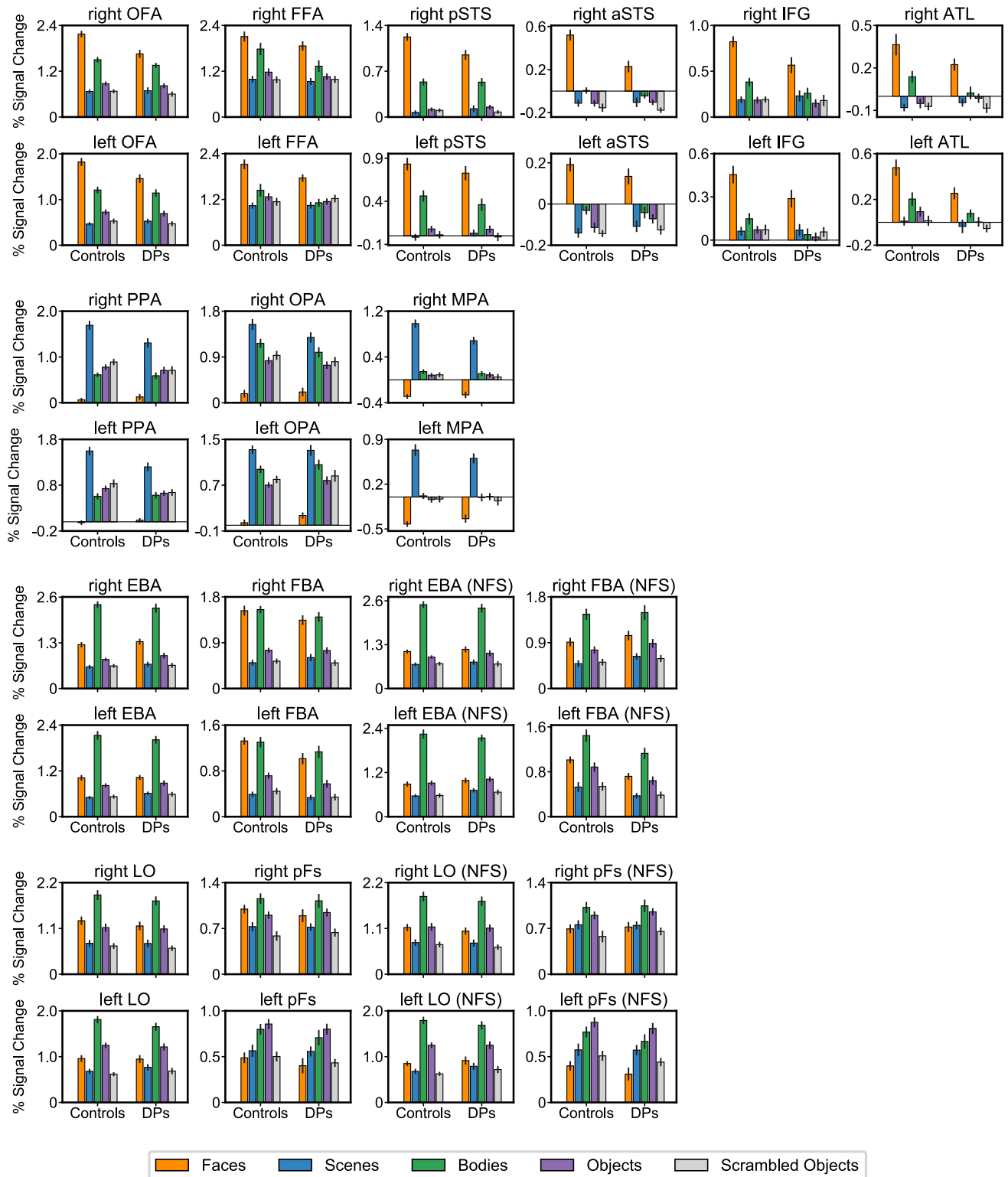
Fig. S9. Responses to all categories in all category-selective ROIs. The top two rows show responses to the five categories in face-selective ROIs; the 3rd and 4th rows display the responses

in scene-selective ROIs; the 5th and 6th rows show responses in body-selective ROIs, including four panels displaying responses to all categories after removing overlapping face-selective voxels at a liberal threshold ($p < 0.05$); the last two rows show the responses in object-selective ROIs, which also includes the panels displaying responses without face-selective voxels ($p < 0.05$). The responses to the non-preferred categories of the DPs and controls were comparable for nearly all non-preferred categories in all ROIs (Tukey Test, $p > 0.05$). The exceptions were in rOFA, where responses to bodies were higher in controls than DPs ($p = 0.042$); in lFBA, where responses to faces were higher in controls than DPs ($p = 0.006$); in lEBA (NFS), responses to scenes were higher in DPs than controls ($p = 0.033$); in lFBA (NFS), responses to faces ($p = 0.001$), bodies ($p = 0.040$), and objects ($p = 0.037$) were higher in controls than DPs. These results provide further evidence that DPs and controls differed in their responses to preferred categories but not non-preferred categories. In addition, the comparable responses to the non-preferred categories indicate DPs' widespread reduced category selectivity was unlikely to be due to reduced input from early perceptual mechanisms. In all panels, error bars stand for ±1 standard error for each group. NFS: Non-face-selective.
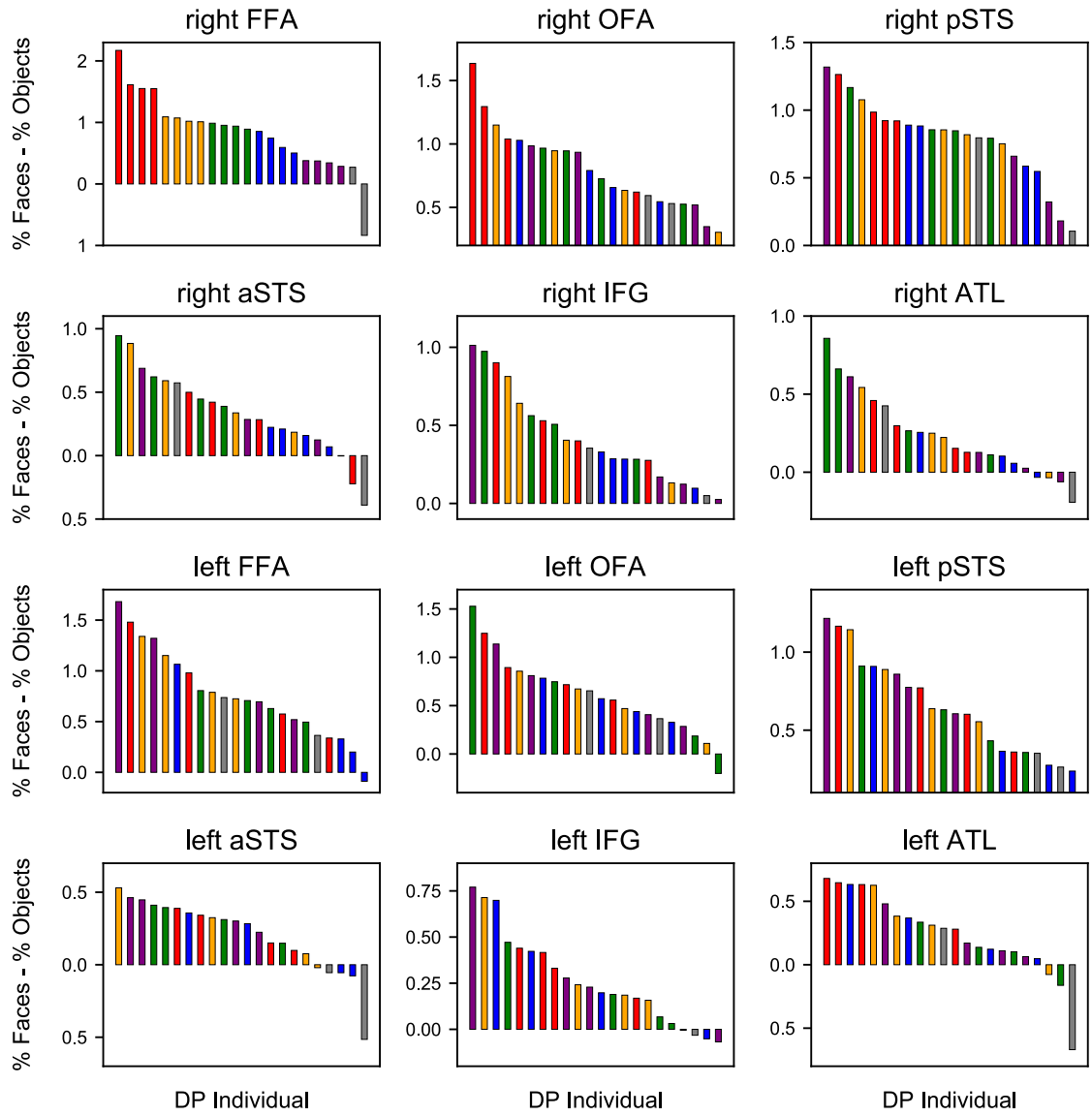
Fig. S10. Individual DP face-selectivity values color-coded based on face-selectivity in right FFA. Individual DP's face-selectivity was first sorted from the largest to the smallest in right FFA and then color-coded using six colors with four individuals in each group for the first five groups and two individuals for the last group. DP face-selectivity values were also sorted from the largest to the smallest in all other face-selective ROIs, but the color coding from the right FFA remained the same. Examination of how individuals in the same color group were distributed in other face-selective ROIs suggests the group differences in face areas did not result from a subset of DPs with extremely low selectivity across different ROIs.
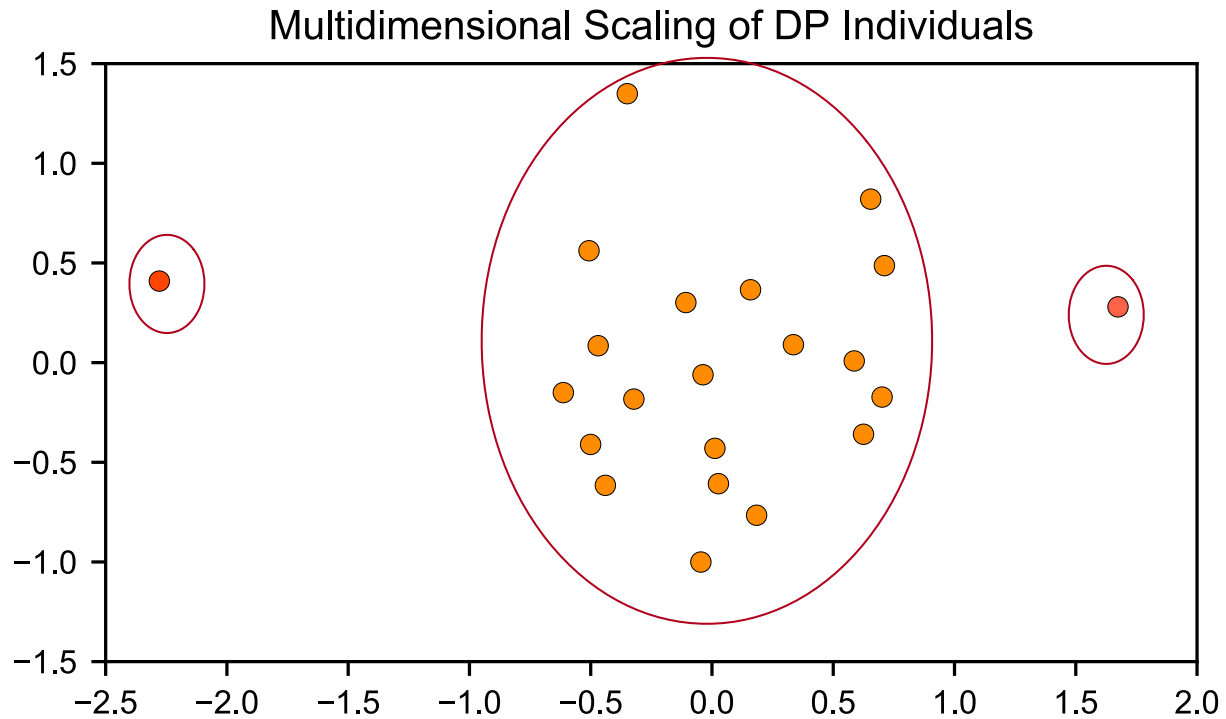
Fig. S11. Clustering result for individual DPs based on their face selectivity in all face-selective ROIs. To investigate whether the DP group contained subtypes, particularly a subtype consistent with the disconnection account, a clustering analysis was carried out with the face selectivity of every face-selective ROIs for each individual. Multidimensional scaling analysis generated one large group, together with two separate individuals. The Calinski-Harabasz index (8) indicated three was the optimal number of clusters in this dataset. The individual on the left had low face selectivity in all face-selective ROIs (to be precise, this individual was presented as the gray bar at position #22, #18, #22, #22, #21, #22, #10, #11, #21, #22, #20, #22 in Fig. S10 left to right, top to bottom panels), and the individual on the right had comparable face selectivity to the controls in all face-selective ROIs (this individual was presented as the red bar at position #1, #1, #2, #7, #7, #5, #2, #13, #9, #6, #8, #4 in Fig. S10 left to right, top to bottom panels), which suggests neither of the two separated individuals was consistent with the disconnection account.

Table S1. Peak coordinates of each functional ROI for controls and DPs.

| Category | ROI | Left Hemisphere | | | | | | Right Hemisphere | | | | | |
| | | Control | | | DP | | | Control | | | DP | | |
		x	y	z	x	y	z	x	y	z	x	y	z
Face	FFA	-40±1	-48±9	-20±2	-40±3	-47±8	-20±3	40±2	-53±5	-17±2	40±2	-48±8	-19±2
	OFA	-40±4	-81±4	-9±6	-37±7	-84±8	-5±7	43±3	-78±5	-7±6	42±8	-78±11	-3±5
	pSTS-FA	-51±5	-53±9	8±4	-51±6	-53±9	9±6	50±5	-47±11	6±4	49±4	-51±9	8±4
	aSTS-FA	-51±4	-5±6	-18±6	-50±4	-5±7	-20±5	53±4	-7±8	-15±7	53±4	-6±8	-18±5
	IFG-FA	-43±4	22±8	9±8	-45±5	21±5	11±5	48±4	22±7	10±8	45±4	18±8	12±7
	ATL-FA	-39±5	-17±6	-29±4	-40±5	-17±8	-29±5	38±6	-5±9	-34±5	38±5	-5±7	-35±4
Body	EBA	-45±2	-74±6	6±4	-45±2	-74±5	7±4	46±3	-69±6	4±7	46±3	-70±7	4±5
	FBA	-41±2	-45±9	-20±4	-40±3	-42±9	-20±4	41±2	-48±7	-16±3	41±3	-46±9	-19±3
Scene	PPA	-24±5	-49±9	-8±3	-25±5	-50±7	-8±4	27±4	-46±7	-9±3	24±6	-51±8	-8±4
	OPA	-31±7	-81±5	22±6	-27±10	-82±6	21±5	33±7	-77±5	26±6	30±10	-79±6	22±5
	MPA	-18±3	-62±6	16±8	-19±2	-62±5	16±9	19±3	-58±3	16±4	18±4	-62±6	20±8
Object	LO	-46±5	-70±7	-4±5	-45±3	-67±7	-3±6	46±4	-68±6	-3±6	45±3	-67±8	-1±8
	pFs	-39±5	-41±6	-19±3	-38±3	-41±6	-19±3	40±4	-43±8	-19±3	39±3	-44±6	-18±3

Table S2. DPs had normal performance in the Leuven Perceptual Organization Screening Test (L-Post). DP #21 did not complete L-Post, but he had normal scores on the low-level visual tests in the Birmingham Object Recognition Battery (BORB)(Tests 2-5). All the DPs who completed the L-Post had scores in the normal range. Each DP had three or fewer subtests in which they were below the 10th percentile (9).

Name of Subtests: 1. RFP Contour Integration; 2. RFP Fragmented Outline; 3. Kinetic object segmentation; 4. Figure–ground segmentation; 5. Fine shape discrimination; 6. RFP Texture Surfaces; 7. Global Motion Detection; 8. Embedded Figure Detection; 9. Recognition of Objects in a Scene; 10. Biological motion; 11. Shape ratio discrimination (Efron); 12. Dot counting; 13. Dot lattices; 14. Recognition of missing parts; 15. Recognition of objects in isolation

DP	1	2	3	4	5	6	7	8	9	10	11	12	13	14	15	No. < 10%	Percentile
1	5	5	5	5	5	4	4	5	5	5	5	4	5	5	5	1	58%
2	4	5	5	5	5	4	4	3	5	5	5	4	4	5	5	1	58%
3	5	5	5	5	5	5	4	3	5	5	5	4	5	5	5	0	100%
4	5	5	5	5	4	5	5	5	5	5	5	5	5	5	5	0	100%
5	5	5	5	5	5	5	4	3	5	5	5	5	5	5	5	0	100%
6	4	5	5	5	5	4	2	5	5	5	5	5	2	5	5	3	16%
7	5	5	5	5	5	5	5	5	5	5	5	5	5	5	5	0	100%
8	5	5	5	5	5	5	4	5	5	5	5	5	5	5	5	0	100%
9	5	5	5	5	5	5	5	4	5	5	5	5	4	4	5	1	58%
10	5	5	5	5	5	5	5	5	5	4	5	5	4	5	5	0	100%
11	5	5	5	5	5	5	4	5	5	5	5	5	4	5	5	0	100%
12	5	5	5	5	5	5	5	5	5	5	5	5	5	5	5	0	100%
13	5	5	5	5	5	5	5	5	5	5	5	4	5	5	5	0	100%
14	-	-	-	-	-	-	-	-	-	-	-	-	-	-	-	-	-
15	4	5	5	5	5	5	5	3	5	5	4	5	5	5	5	1	58%
16	5	5	5	5	5	5	5	5	5	5	4	5	5	5	5	1	58%
17	5	4	5	5	5	4	4	5	5	5	4	5	5	5	5	3	16%
18	5	5	5	5	5	5	5	5	5	5	5	5	5	5	5	0	100%
19	-	-	-	-	-	-	-	-	-	-	-	-	-	-	-	-	-
20	5	5	5	5	4	5	4	5	5	5	5	5	5	5	5	0	100%
21	-	-	-	-	-	-	-	-	-	-	-	-	-	-	-	-	-
22	5	5	5	5	5	5	4	5	5	5	5	5	5	5	5	0	100%
< 10% Cut-Off	3	4	4	4	3	4	3	2	4	2	4	3	3	4	4	-	-

References

1. Ojemann JG, et al. (1997) Anatomic Localization and Quantitative Analysis of Gradient Refocused Echo-Planar fMRI Susceptibility Artifacts. *NeuroImage* 6(3):156–167.

2. Kay K, Rokem A, Winawer J, Dougherty R, Wandell B (2013) GLMdenoise: a fast, automated technique for denoising task-based fMRI data. *Front Neurosci* 7:247.

3. Norman-Haignere S, et al. (2016) Pitch-Responsive Cortical Regions in Congenital Amusia. *J Neurosci* 36(10):2986–2994.

4. Hagler DJ, Saygin AP, Sereno MI (2006) Smoothing and cluster thresholding for cortical surface-based group analysis of fMRI data. *NeuroImage* 33(4):1093–1103.

5. Power JD, Barnes KA, Snyder AZ, Schlaggar BL, Petersen SE (2012) Spurious but systematic correlations in functional connectivity MRI networks arise from subject motion. *Neuroimage* 59(3):2142–2154.

6. Duchaine B, Yovel G, Nakayama K (2007) No global processing deficit in the Navon task in 14 developmental prosopagnosics. *Soc Cogn Affect Neurosci* 2(2):104–113.

7. Duchaine B, Germine L, Nakayama K (2007) Family resemblance: Ten family members with prosopagnosia and within-class object agnosia. *Cogn Neuropsychol* 24(4):419–430.

8. Caliński T, Harabasz J (1974) A dendrite method for cluster analysis. *Commun Stat* 3(1):1–27.

9. Crawford JR, Garthwaite PH, Slick DJ (2009) On percentile norms in neuropsychology: proposed reporting standards and methods for quantifying the uncertainty over the percentile ranks of test scores. *Clin Neuropsychol* 23(7):1173–1195.